https://ntrs.nasa.gov/search.jsp?R=19830023279 2020-03-21T03:34:29+00:00Z

General Disclaimer

One or more of the Following Statements may affect this Document

- This document has been reproduced from the best copy furnished by the organizational source. It is being released in the interest of making available as much information as possible.

- This document may contain data, which exceeds the sheet parameters. It was furnished in this condition by the organizational source and is the best copy available.

- This document may contain tone-on-tone or color graphs, charts and/or pictures, which have been reproduced in black and white.

- This document is paginated as submitted by the original source.

- Portions of this document are not fully legible due to the historical nature of some of the material. However, it is the best reproduction available from the original submission.

Produced by the NASA Center for Aerospace Information (CASI)

NASA TECHNICAL MEMORANDUM

NASA TM-77213

CARBON LINES AT LIMITEDLY LOW FREQUENCIES

I. Ye. Val'tts

Translation of "Uglerodnyye linii na predel'no nizkikh chastotakh," USSR Academy of Sciences Space Research Institute Report Pr-758, Moscow, 1983, pp. 1-56.

(NASA-TM-77213) CARBON LINES AT LIMITEDLY LOW FREQUENCIES (National Aeronautics and Space Administration) 44 p HC A03/MF A01 CSCL 03A

N83-31550

Unclas
G3/89 28395

NATIONAL AERONAUTICS AND SPACE ADMINISTRATION
WASHINGTON, D.C. 20546 MAY 1983

ORIGINAL PAGE IS
OF POOR QUALITY

STANDARD TITLE PAGE

1. Report No.	2. Government Accession No.	3. Recipient's Catalog No.
NASA TM-77213		

4. Title and Subtitle	5. Report Date
CARBON LINES AT LIMITEDLY LOW FREQUENCIES	MAY 1983
	6. Performing Organization Code

7. Author(s)	8. Performing Organization Report No.
I. Ye. Val'tts	
	10. Work Unit No.

9. Performing Organization Name and Address	11. Contract or Grant No.
Leo Kanner Associates Redwood City, CA 94063	NASW-3541
	13. Type of Report and Period Covered
	Translation
12. Sponsoring Agency Name and Address	14. Sponsoring Agency Code
National Aeronautics and Space Administration, Washington, D.C. 20546	

15. Supplementary Notes

Translation of "Uglerodnyye linii na predel'no nizkikh chastotakh," USSR Academy of Sciences Space Research Institute Report Pr-758, Moscow, 1983, pp. 1-56.

16. Abstract

Detection of several absorption recombination radio lines of carbon at 26 MHz in Cas A direction resulted in an attempt to select similar situations (a gas cloud projection on the intense source of the nonthermal radio emission) that are promising for detecting lines of such a kind. Recommendations are given for observations to be made.

17. Key Words (Selected by Author(s))	18. Distribution Statement
	Unclassified--Unlimited

19. Security Classif. (of this report)	20. Security Classif. (of this page)	21. No. of Pages	22.
Unclassified	Unclassified		

CARBON LINES AT LIMITEDLY LOW FREQUENCIES

I. Ye. Val'tts

Introduction

In 1980 the Khar'kov UTR-2 radio telescope detected radio frequency absorption lines from a powerful Cas A radiation source. /3* The observed frequency was 26.13 MHz. The parameters obtained from the observations made it possible to interpret this line as a transition in the ultrafine structure of the ^{14}N nitrogen atom [1], or the dielectronic recombination of heavy elements in the hot interstellar medium [2], or as the recombination of the C631α carbon atom in cold, slightly ionized gas [2]. The last idea seemed most likely, although it required confirmation, such as by observations of similar recombination lines at adjacent frequencies. These observations were made in 1981 [3, 4], and the discovery of C640α and C630α lines reliably confirmed that a number of carbon radiorecombination lines are found emitted from a cloud of slightly ionized gas in the line of sight towards Cas A.

Theoretically the 10-meter wavelength range has certain advantages for detecting lines of this kind. In fact, with deviations from MGP, which apparently occur in interstellar space, the intensity of radiorecombination lines depends strictly on changes in the ratio $\Delta b_n/b_n$ /4 (i.e., on the slope of the derivative function $\Delta b_n/b_n$ of n). Shaver's calculations [5] indicate that the intensity of the lines seen in radiation at frequencies $\sim$1000 MHz should increase up to 100-200 MHz (with a maximum in the $\sim$150 MHz frequency range), then subside so as to reach a maximum in absorption at frequencies of 20-30 MHz. The transition from radiation to absorption occurs in the frequency range $\sim$40 MHz, and at these frequencies the lines should be extremely weak. It is interesting to note that, although detection of absorption lines at 26 MHz corroborates Shaver's theoretical estimate [5], the absence of radiation lines at 150 MHz [6, 7] points out possible defects in the theory. Walmsley and Watson [8] recently offered new theoretical calculations which may better explain the features of absorption components in the direction of Cas A. These calculations are based on the assumption that the gas forming the observed lines has a very low electron density. Some process resembling dielectronic recombination plays a special part in the repopulation of higher energy levels of the carbon atom here. These calculations are, however, in need of serious theoretical and experimental proof.

In view of the successful experiment at 26 MHz it would be interesting to continue research in this direction. Of unquestionable interest are such cases as when a gas layer or cloud is projected onto a powerful source of nonthermal radio frequency emissions (a situation similar to that of Cas A). The choice of such situations can proceed

---

*Numbers in the margin indicate pagination in the foreign text.

in the following directions:

powerful galactic radio emission sources -- interstellar gas; /5

powerful extragalactic radio emission sources -- the interstellar gas of our galaxy;

powerful extragalactic radio frequency sources -- intergalactic gas at astronomical distances, possibly belonging to other galaxies projected into the line of sight.

Here we should be guided by the following considerations stemming from the conditions of the UTR-2 experiment. The ratio of T_L to T_C for the detected C631α line is $\sim 2 \times 10^{-3}$ [3]. The signal collection time was 10 hrs at a resolution of 2 kHz. The flux from Cas A at 26 MHz $F_{26} \approx 5 \times 10^4$ W/m^2·Hz. With the expected absorption layer parameters, over a month of continuous observations apparently is needed for accumulating this kind of signal ($\sim 2 \times 10^{-3}$), if the base flux is 10 times less than the flux from Cas A. At 26 MHz, as shown by the results of the UTR-2 examination [9-12] and that of the Clark Lake Observatory telescope [13], the fluxes of more powerful radio sources lie within the range of ($10^2 < F_{26} < 10^3$) flux units. It is impossible here to reduce the signal accumulation time by increasing resolution, since the real line width is $\lesssim 2$ kHz, as demonstrated by subsequent studies on varying resolution [14]. However, the signal-to-noise ratio in the experiment [3] exceeded the noise track by more than 20 times (see fig. 1a). If we decide on a value of 3σ, for sources of $F_\nu \gtrsim 100J$ the accumulation time comes within 1 month for telescopes of the UTR-2 type, i.e., radio sources with fluxes $F_\nu \lesssim 100J$ have no meaning as a base.

Such a substantial restriction on the flux density of radio /6
sources acting as a base is imposed by background radiation from our galaxy, which at these frequencies is about 3×10^4 °K (see, for example, [15]). If we assume that the effective area of the UTR-2 is $S_{eff} = 2 \times 10^4$ m^2, the antenna temperature from extragalactic radio sources with small angular dimensions (≈1") would be on the order of the background T_A, i.e., 3×10^4 °K, if the flux from the source is ≈1000J. The background radiation at these frequencies can itself act as a base if there is a close enough gas-dust complex covering the antenna pattern in angular size. We shall discuss this question in more detail below.

Thus the setup of the experiment to systematically observe sources of continuous radiation for carbon absorption lines is ineffective. Only in certain isolated cases, with a powerful enough base and direct indications that there is cold, slightly ionized gas in the line of sight, is it possibly worthwhile undertaking a search for lines of this sort.

ORIGINAL PAGE IS
OF POOR QUALITY

For this reason we shall discuss first of all the most powerful radiation sources, those whose flux is comparable to that from Cas A. Among these sources are: remnants of the Crab Nebula and Vela XYZ supernovae, the Hydra A, Virgo A, Hercules A, Cygnus A, and Centaurus A radiogalaxies, and the radiation source in the center of our galaxy, Sgr A.

The presence of a carbon cloud in the line of sight towards this source is indicated by HI absorption lines ($\lambda \approx 21$ cm) and, what is /7 much more essential, molecular radio lines, since C^+ zones obviously are linked directly to dense molecular clouds (see, for instance, [16] and [17]), the carbon line velocities coinciding, as a rule, with those of the molecular lines (see fig. 2). (In figs. 1b and 1c we reproduce the profiles of molecular lines observed in the direction of Cas A [18, 19].)

Furthermore, as was noted in [20], the shape of the 21 cm HI absorption line profile is, as a rule, very complex, introducing some ambiguity into analysis of certain HI line features. The molecular profiles normally are much narrower than the HI profiles and the neutral gas collection rates often are better determined from observations of molecular lines. We now offer the following data on HI line and OH and CO molecular lines in the direction of the powerful radio sources mentioned above.

The Tau A ($\theta = 3.6'$ [21]; $F_{26} \approx 2829$ [13]) and Cyg A (double radiogalaxy with complex structure; spacing between two main components $\lesssim 2.0'$ -- see, for example, [22]; $F_{26} \approx 31184J$ [13]), radio sources, like Cas A, lie close to the plane of the galaxy. The line of sight towards them intersects the arm of Perseus, from which C630α, C631α, and C640α lines were detected in [1], [3], and [4]. Using the Owens Valley Observatory interferometer, Greisen [21] obtained a detailed spectrum of neutral hydrogen in the direction of Tau A and Cyg A -- and these spectra are shown in Fig. 3 and fig. 4a & 4b. The physical conditions in the clouds of molecular gas projecting on Tau A and Cyg A have been studied by Davies and Matthews [18], among others, using the Mk I and Mk II telescopes at the Jodrell Bank /8 Observatory. We have taken the comparative characteristics of the molecular clouds in the direction of Cas A and Cyg A from [18] and reproduced them in table 1. As this table shows, the strongest features of the OH and HI absorption lines in the direction of Tau A and Cyg A are several times weaker than the strongest features of lines in the direction of Cas A. The profiles of 21 cm lines in the direction of Cas A and Cyg A were also compared using the Bonn 100 m telescope [24] -- see fig. 4c. The carbon lines in Cas A are formed in the arm of Perseus ($V \approx -40$ km/sec); the major part of the arm of Perseus is not projected on Tau A [23]; the corresponding projection on Cyg A has a velocity of $V \approx -85$ km/sec).

Thus to accumulate carbon lines in the direction of Tau A and Cyg A we need to significantly increase the integration time -- and it should be noted here that increasing the integration time in Cas A observations should reveal the weaker features of the carbon lines, the same as would appear in observations of Tau A and Cyg A. The

most recent review of extragalactic radio sources in the HI 21 cm line [25] indicated the presence of a very slight accumulation of gas in the direction of Cyg A -- see fig. 4d.

With regard to the nature of the molecular clouds, in [18] it is noted that the absorbing gas in the direction of Cas A, Cyg A, and Tau A has extremely similar characteristics, typical of a cold, slightly ionized medium. This, of course, increases the likelihood of finding carbon lines in the direction of Cyg A and Tau A.

Hydra A, Virgo A, and Hercules A are powerful radio sources whose /9
significant low-frequency flux (F_{26}Hyd A ≈ 1900 Jy [11]; F_{26}Vir A ≈ 4750 Jy [9]; F_{26}Her A ≈ 2084 Jy [10]) provides an opportunity to detect absorption lines in the clouds projecting on them. Extragalactic radio sources were viewed at Nantes [25] and Arecibo [26] in a special attempt to find exact projections of the galactic gas accumulations on a source of continuous radiation -- the HI 21 cm line here being in absorption. Very weak absorption was detected in the direction of Her A in [25] -- see figs. 5a and 5b. In [27] and [28], work involving a higher sensitivity than in [25], weak absorption was also found in Hyd A (figs. 6a, 6b) and Vir A (fig. 7). Note that the Vir A radio source is located at a very high galactic latitude: $b^{II} = 75°$. An attempt to detect an OH absorption line in the direction of Her A proved futile [29].

The remnants of the Vela XYZ supernova and the Cen A radiogalaxy are sources with large negative accumulation and inaccessible for observations from the northern radio telescopes at Grakovo and Clark Lake. The following can basically be said about these objects: Vela XYZ has larger angular dimensions -- 240' [21] -- which exceed the pattern of radio telescopes at frequencies of 20-30 MHz. Thus if there is a cloud of interstellar gas covering part of the Vela XYZ nebula, its considerable integral flux (2300 Jy at 400 MHz [21]) produces a much lesser effect, conforming to the ratio $\Omega_{antenna}/\Omega_{source}$. Hence the situation in the direction of Vela XYZ would be markedly worse than in the direction of the Crab Nebula. /10

The Cen A radiogalaxy has frequently been studied in the HI 21 cm absorption lines; the most recent work of this kind was done with the RATAN-600 radio telescope by Gosachinskiy et al. [30]. The observations revealed a total absence of the absorption line features of HI formed in the interstellar gas of our galaxy. A very weak feature was obtained in [28] -- see fig. 8. Study of Cen A in molecular lines also provided no indication of accumulated gas in this direction: special work was done in 1975 to ascertain the possible molecular nature of the dark gas-dust band projected on Cen A by absorption in the formaldehyde line [31]. No galactic or extragalactic H_2CO absorption features were detected, although in 1976 the Parks 64 m telescope found a formaldehyde absorption line at 6 cm belonging to galaxy NGC 5128 [32].

The molecular lines of a powerful nonthermal radio source (F_{26} ≈ 500 Jy -- extrapolated from data in [21]) of small angular size (θ ≈ 3' [21]) in the center of our galaxy have been studied quite often.

A detailed map of the distribution of ionized gas in the direction of Sgr A is given in [33] and elsewhere. According to radio interferometer studies in molecular lines, obtained at the Owens Valley Observatory [34], two dense molecular clouds with radial velocities of +25 km/sec and +45 km/sec are found in the direction of Sgr A. The presence of these two molecular clouds in the details is confirmed by observations in the emission lines of CO [35] and NH_3 [36] and in the absorption line of H_2CO [37]: the OH clouds coincide with the CO /11
clouds with regard to velocity and position in space [34]. The rich molecular spectrum of the center of the Galaxy apparently provides enough basis for predicting a possible detection of low-frequency carbon recombination lines. Because the Sgr A radio source is weak in comparison with Cas A, however, work with a telescope like the UTR-2 is highly laborious.

We now turn to less powerful radio sources.

At the low frequencies of interest to us (26 MHz), the only powerful radio sources in our galaxy are the remnants of supernovae, since they have continuous radiation spectra which grow towards low frequencies. Downes' catalog of supernova remnants [21] contains data on fluxes at frequencies of 400, 1400, and 5000 MHz, angular and linear dimensions, and distances to sources. Based on the spectral index values and data on flux given in [21] we can distinguish over 20 remnants of supernova explosions whose fluxes at 26 MHz can reach $\approx 10^3 J$. The angular size of the sources is very large (>1°) in most cases, however. Point objects are suitable for our purposes: the Tycho Brahe supernova remnant ($F_{26} \approx 500 J$) and W 66 ($F_{26} \approx 5000 J$). Their characteristics, taken from Downes' catalog [21], are given in table 2, column 5. The characteristics of Cas A [21] are also given here for comparison. This table includes two radio sources in the southern sky, KE 19A and KE 47, which have pertinent fluxes and sizes. The radio-structure of the Tycho Brahe supernova remnant (ZS 10) has been extensively studied at 21 cm and other wavelengths [38, 39]. The HI /12
21 cm absorption line profile obtained at Nantes [27] is shown in fig. 9a. A weak 1667 MHz OH line absorption was observed in the direction of ZS 10 [40] -- see fig. 9b.

The gas complex in the constellation Cygnus relating to supernova remnant W 66 (*DR* 4, γCyg, G 78.2 + 1.8) is extraordinarily rich in thermal and nonthermal radio sources, H II zones, star formation regions, and molecular clouds. Detailed description of this region, maps, and the physical parameters of various sources are given in [41]. There are no data available on the projection of the molecular cloud on the remnants of SN W 66, however.

Perhaps more promising are the remnants of SN of larger angular size, which virtually cover the radio telescope's pattern. Among such remnants are IC 443 ($F_{26} \approx 850 J$) and W 44 ($F_{26} \approx 1000 J$) -- see table 2. Observations were done in [42] on the lines of the molecular cloud almost completely covering the entire remnants of SN IC 443; there are molecular clouds in the environs of W 44 as well [43]. One

complication is that the carbon zones themselves generally have very small linear, and thus angular dimensions -- on the order of several minutes of arc. The absorption effect can be anticipated only if several C II zones are projected an SN remnant of this kind.

We now turn to the next class of objects -- extragalactic sources on which galactic gas is projected. As mentioned above, radio sources with fluxes of $\approx 1000J$ can be treated as bases. But radio sources with /13 fluxes of $\approx 100J$ at 26 MHz are classified as bright enough and can serve to reveal absorbing masses of gas at higher frequencies. These sources thus can be used to reveal gas-dust complexes which are promising for observations of galactic background absorption.

Table 3 shows the sources with $\delta > -13°$ from the catalogs of Braude et al. [9-12] and Viner and Erickson [13] which have sources at 26 MHz with >200 J. These data are not complete, in that the published observations from Grakovo [9-12] include surveys in the $-13° < \delta < +20°$ range, while those from Clark Lake are between $3°20' < \delta < 63°20'$.

The data on observations at the 21 cm HI line, shown in table 2 and fig. 10, were taken from surveys of extragalactic radio sources [25, 26] which were, as mentioned above, special attempts to find precise projections of galactic gas accumulations on a source of continuous radiation, the 21 cm HI line here being in absorption. Figure 10 depicts the emission and absorption profiles of the 21 cm HI line in the direction of the radio sources which are brightest at 26 MHz (according to data in [25]). Figure 11 shows separate profiles of 21 cm HI lines for ZS 84, ZS 111, ZS 123, and ZS 353 taken from [27].

Similar surveys were done at Nantes in the OH [44] and CO 2.6 mm lines, at Kitt Peak [45], and at Fort Davis [47] in the direction of a few radio sources with particularly strong 21 cm HI absorption lines done in order to reveal possible HI-OH-CO correlations.

Column 6 in table 3 shows the amount of relative absorption $A = 1 - e^{-\tau}$ in the 21 cm HI line for some of the strongest features, /14 using data from the Nantes survey [25]. A dash indicates absence of absorption. Columns 7-9 and 10-12 show data on absorption in the 1667 MHz OH line [40, 44] and on CO emission at 2.6 mm [45]; see also figs. 12 and 13a & b. The brightest molecular line features are found in the direction of radiogalaxy ZS 111.

The OH lines are significantly weaker in the direction of the strongest sources in table 3 -- ZS 123 and ZS 353 (we do not include data on observations of molecular lines in the direction of radiogalaxy Per A).

Many clouds of cold (100-150 K) gas and dark regions are seen [46] on the Palomar atlas near the position of the radio source [44, 45]. The HI, OH, and CO line profiles are shown in figs. 10-13. The central velocities of the OH and CO lines are quite close [45]. The CO

line is wide and reflects the binary structure of the radio source [48]. A similar effect is visible in OH lines [44].

ZS 123 is one of the strongest radiogalaxies. A detailed map of a 1.5° X 1.5° region, including ZS 123 at a frequency of 1420 MHz, was obtained by a 100-meter radio telescope [49]. Study of the dark clouds of this region on the Palomar atlas maps revealed that ZS 123 lies in the area of the Taurus complex [45]. The OH and CO molecular lines, as in the case of ZS 111, are complex in structure -- see figs. 13b, 14a & b, and 15.

CO emission was found at a distance of 120' from the source, which corresponds to a distance of 200 ps from a cloud measuring 14 ps [48]. A cloud of this size should be in the fragmentation stage -- and this /15 may also be reflected in the structure of the CO line. The two main components of the ^{13}CO line coincide in velocity with the OH and H_2CO lines [48].

The publications we reviewed held no detailed description of the ZS 353 radio source, possibly of interest to us because of the flux which is significant at low frequencies (see table 3). This source has been extensively studied in the HI, OH, CO, and H_2CO lines -- see figs. 10, 11, 13b, 15 and 16. Despite the presence of absorption features in the direction of ZS 353, the gas complex projected on this source apparently is less powerful than in the direction of ZS 111, as in the case of ZS 353. We should note, however, that the optical depth of the OH features in the direction of Cas A (see fig. 1b & c) is no greater than in the direction of ZS 123 and ZS 353, and even less than in the direction of ZS 111. The gas complex in the direction of ZS 111, which contains molecular clouds, may possibly provide carbon absorption lines with the galactic background serving as the base.

One other possible combination of absorbing gas and powerful source of radiation as a base which we are prepared to discuss in this paper is a quasar or radiogalaxy projecting on intergalactic clouds of gas. In such a case radiorecombination absorption lines would help reveal accumulations of intergalactic gas which would not manifest themselves unless they absorbed the flux from a background source passing through them. As a rule, quasars with large z_e ($\gtrsim 2$) have rich absorption spectra, indicating the presence of gas accumulations/16 in the direction of the source. Of the 1549 quasars and objects of the BL Lac type included in the latest optical catalog of such sources [50], 111 have absorption systems. But not all quasars whose spectra contain absorption line systems emit radio waves; only 60 of the 111 do. Of these, 48 have flux $F_\nu \gtrsim 1$ at intermediate frequencies -- see [51], for example. The flux at lower frequencies normally rises no more than 10 times in such cases. Among these 48 sources is PKS 0237-23, which has one of the richest absorption spectra -- over 200 features; OQ 172 ($z_e = 3.53$) and OH 471 ($z_e = 3.402$) are the most remote of the known quasars; two sources (of 5) in the direction of which intergalactic absorption lines of neutral hydrogen with $\lambda = 21$ cm

have been discovered are the BL Lac-type object AO 0235+164 and the quasar 1331+164. Table 4 presents data on the radio quasars with absorption spectra which are most powerful at low frequencies: the name of the object, the minimum frequency at which the source is observed, and the flux corresponding to this frequency. The notes mention objects in whose direction a 21 cm line is detected. As can be seen from table 4, the fluxes are too low, and the carbon line cannot be detected with such a weak lighting. The exception is quasar ZSR 9, which has a strong enough flux ($F_{26} = 100J$) and an absorption system ($z_a = 1.6245$) formed by hot gas in which the carbon line may be intensified by dielectronic recombination. We discussed a situation similar to this in [52].

The search for intergalactic cloud projections on radiogalaxies proved inconclusive [53-55]. (An exception may be the relatively /17 unknown cloud in the galaxy group NGC 1023 [56].) HI, CO, and OH lines, radiorecombination lines observed both in emission and absorption in the direction of certain radiogalaxies (see [57-60], for instance), relate to the distribution of gas in the structure of the galaxies themselves, and have no bearing on the study of intergalactic gas-dust complexes.

Finally, we shall examine the possibility of detecting carbon absorption lines when the galactic background serves as the base. From Lynds' catalog [61] we selected 23 dark regions meeting the following requirements: $\delta \gtrsim -10°$; size $>1°$; degree of opacity, according to Lynds, 4, 5, 6. About the same degree of opacity is shown by dark clouds from which carbon radiorecombination lines have been detected at high frequencies -- ζ Oph, for example. The parameters and coordinates of these regions are given in table 5. We can distinguish six major zones, three of which in the longitude regions $l^{II} \approx 20°$, $l^{II} \approx 30°$, and $l^{II} \approx 52°$ join with the plane of the Milky Way and three in the longitude regions $l^{II} \approx 160°$, $l^{II} \approx 170°$, and $l^{II} \approx 205°$ (Ori) represent isolated complexes.

Carbon lines are normally produced by Class B stars; several indirect indications can reveal the presence of such stars in a gas-dust complex: reflecting nebulae are created around class B stars in dense clouds; furthermore, some of the star's energy is released in the infrared region. Columns 9 and 10 contain the coordinates of IR sources in the $\approx 4\mu$ range, taken from catalog [62]; column 11 contains the designation of the reflecting nebula which may be associated with the given dark cloud. Data on the projections of reflecting nebulae /18 on the dark clouds are taken from the reflecting nebula catalog [63].

Since the background antenna temperature was about 30 times lower than the antenna temperature from Cas A at 26 MHz, the time to collect features from regions with physical parameters such as those in the direction of Cas A rises significantly. Apparently more promising are observations at ≈ 16 MHz, where the T_B of the background $\approx 10^5$°K. In this case the accumulation time remains in the neighborhood of 10 hours.

Conclusions

Hence through successful observations of many radio-frequency absorption combination lines in Cas A with the Kharkov UTR-2 telescope (frequency ≈26 MHz) we have estimated the possibility of detecting similar lines in the direction of other continuous radiation sources at low-frequency range antennas in general, and specifically the UTR-2. We have examined projections of galactic (supernova remnant) and extragalactic radio sources on the gas clouds of our galaxy and projections of the "quasar-intergalactic gas accumulation" type. The criteria used to select the most promising situations were the following signs: a) the presence of a flux at 26 MHz >100 f; b) the presence of OH and, if possible, CO absorption lines. A carbon line should be expected, obviously, at approximately the same velocities that correspond to the OH and CO features.

The following conclusions can be made. The masses of gas projecting on the Crab Nebula and radiogalaxy Cyg A, as the observations of OH, CO, and H_2CO lines imply, are much smaller than those projecting on Cas A. Thus accumulating carbon lines in the direction of Tau A and Cyg A obviously is equivalent to accumulating weaker features from Cas A. Nevertheless, in view of the similarity of gas clouds in the direction of Tau A, Cyg A, and Cas A, the situation with regard to the Tau A and Cyg A radio sources is rather promising. /19

No significant accumulations of gas have been found in the direction of Vir A or Her A.

From the Northern Hemisphere supernova remnants, other than Tau A, we cannot preclude the possibility of detecting carbon lines in the direction of SNR Tycho Brahe, W 66, IC 443, and W 44 which are appropriate in strength and size. But, judging by the OH features, the gas cloud in the direction of SNR Tycho Brahe is not very large, and W 66 has not been studied in molecular lines, so recommendations about this source would obviously be premature. The angular sizes of IC 443 and W 44 may markedly exceed those of the C II zones.

Among the gas complexes projecting on extragalactic radio sources we can distinguish the one in the direction of ZS 111, although ZS 111 is a very weak base; observations of gas complexes in the direction of more powerful radio sources -- ZS 123 and ZS 353 -- appear more promising.

Absorption of galactic background radiation in carbon lines obviously is more effective at frequencies somewhat below 26 MHz. A number of dark regions have been selected in which background absorption might be expected.

No accumulations of intergalactic gas have yet been found to project on powerful radiogalaxies or quasars. An exception may be quasar ZSR 9, the situation with which was discussed in another paper [52].

REFERENCES

1. Konovalenko, A. A., and L. G. Sodin, Nature 283, 360 (1980).

2. Blake, D. H.,R. W. Crutcher, N. D. Watson, Nature 287, 707 (1980).

3. Konovalenko, A. A., and L. G. Sodin, Pis'ma v AZh 7, 402 (1981).

4. Konovalenko, A. A., and L. G. Sodin, Nature 294, 135 (1981).

5. Shaver, P. A., Astron. and Astrophys. 49, 1 (1976).

6. Casse, J. L., and P. A. Shaver, Astron. and Astrophys. 61, 805 (1977).

7. Shaver, P. A., A. Pedlar, R. D. Davies, Monthly Notices of R.A.S. 177, 45 (1976).

8. Walmsley, C. M., and W. D. Watson, Astrophys. J. 255, L123 (1982).

9. Braude, S. Ya., A. P. Miroshnichenko, K. P. Sokolov, N. K. Sharykin, Astrophys. and Space Sci. 54, 3 (1978).

10. Braude, S. Ya., A. P. Miroshnichenko, K. P. Sokolov, N. R. Sharykin, Astrophys. and Space Sci. 64, 73 (1979).

11. Braude, S. Ya., A. P. Miroshnichenko, K. P. Sokolov, N. R. Sharykin, Astrophys. and Space Sci. 74, 409 (1981).

12. Braude, S. Ya., A. P. Miroshnichenko, K. P. Sokolov, N. R. Sharykin, Astrophys. and Space Sci. 76, 279 (1981).

13. Viner, M. R., and W. C. Erickson, Astron. J. 80, 931 (1975).

14. Konovalenko, A. A., private communication.

15. Cane, H. V., Austr. J. Phys. 31, 561 (1978).

16. Brown, R. L., in "Radio recombination lines," Proc. of a Workshop Held in Ottawa, Canada, Aug. 24-25, 1979 (Ed. by P. A. Shaver), Dordrecht, etc., Reidel, 1980, p. 127.

17. Chaisson, E. J., Astrophys. J. Letters 197, L65 (1975).

18. Davies, R. D., and H. E. Matthews, Monthly Notices of R.A.S. 156, 253 (1972).

19. de Jager, G., D. A. Graham, R. Wielebinski, R. S. Booth et al., Astron. and Astrophys. 64, 17 (1978).

20. Chaisson, E. J., Astron. J. 79, 555 (1974).

21. Downes, D., Astron. J. 76, 305 (1971).

22. Hargrave, P. J., and M. Ryle, Monthly Notices of R.A.S. 166, 305 (1974).

23. Greisen, E. W., Astrophys. J. 184, 379 (1973).

24. Mebold, U., and D. L. Hills, Astron. and Astrophys. 42, 187 (1975).

25. Crovisier, J., I. Kazes, D. Aubry, Astron. and Astrophys. Suppl. Ser. 32, 205 (1978).

26. Crovosier, J., I. Kazes, D. Aubry, Astron. and Astrophys. Suppl. Ser. 41, 229 (1980).

27. Lazareff, B., Astron. and Astrophys. 42, 25 (1975).

28. Hughes, M. P., A. R. Thompson, R. S. Colvin, Astrophys. Journ. Suppl. Ser. 23/200, 323 (1971).

29. Kazes, I., J. Crovisier, D. Aubry, Astron. and Astrophys. 58, 403 (1977).

30. Gosachinskiy, I. V., V. G. Grachev, N. F. Ryzhkov, Astron. zh. 57, 1121 (1980).

31. O'Connell, R. W., W. C. Saslaw, B. E. Turner, Monthly Notices of R.A.S. 170, 29 (1979).

32. Gardner, P. P., and J. B. Whiteoak, Monthly Notices of R.A.S. 175, 9P (1976).

33. Pauls, T., and P. G. Mezger, Astron. and Astrophys. 44, 259 (1975).

34. Bieging, J. H., Astron. and Astrophys. 51, 289 (1976).

35. Solomon, P. M., N. Z. Scoville, A. A. Penzias, R. W. Wilson et al., Astrophys. J. 178, 125 (1972).

36. Knowles, S. H., and A. C. Cheung, Astrophys. J. 164, L19 (1971).

37. Fomalont, C. B., and L. N. Weliachew, Astrophys. J. 181, 781 (1973).

38. Williams, D. R. W., Astron. and Astrophys. 28, 309 (1973).

39. Dulin, R. M., and R. G. Strom, Astron. and Astrophys. 39, 33 (1975).

40. Nguyen-Q-Rieu, A. Winnberg, J. Guilbert, J. R. D. Lepine et al., Astron. and Astrophys. 46, 413 (1976).

41. Goudis, C., Astrophys. and Space Sci. 44, 281 (1976).

42. Cornett, R. H., G. Chin, G. R. Knapp, Astron. and Astrophys. 54, 889 (1977).

43. Pashchenko, M. I., Pis'ma v AZh 1, 23 (1975).

44. Dickey, J. M., J. Crovisier, I. Kasez, Astron. and Astrophys. 98, 271 (1981).

45. Kasez, I., and J. Crovisier, Astron. and Astrophys. 101, 401 (1981).

46. Dickey, J. M., E. E. Salpeter, Y. Terzian, Astron. and Astrophys. Suppl. Ser. 36, 77 (1978).

47. Liszt, H. S., and W. B. Burton, Astrophys. J. 228, 105 (1979).

48. Combes, F., E. Falgarone, J. Guilbert, Nguyen-Q-Rien, Astron. and Astrophys., 90, 88 (1980).

49. Reich, W., P. Kalberla, J. Neidhöffer, Astron. and Astrophys. 52, 151 (1976).

50. Hewitt, A., and G. Burbidge, Astrophys. J. Suppl. Ser. 43, 57 (1980).

51. Kühr, H., A. Witzel, I. I. K. Pauliny-Poth, U. Nauber, Astron. and Astrophys. Suppl. Ser. 45, 367 (1981).

52. Val'tts, I. Ye., in preparation.

53. Morton, R. M., and D. G. Steigerwald, Astrophys. J. 217, 883 (1977).

54. Lo, K. Y., and W. L. W. Sargent, Astrophys. J. 227, 756 (1979).

55. Davies, R. D., Phil. Trans. Roy. Soc. London A296/1419, 407 (1980).

56. Hart, L., R. D. Davies, S. C. Johnson, Monthly Notices of R.A.S. 191, 269 (1980).

57. Rots, A. H., Astron. and Astrophys. Suppl. Ser. 41, 189 (1980).

58. Weliachew, L., Astrophys. J. 167, L47 (1971).

59. Gardner, F. F., and J. B. Whiteoak, Nature 247, 526 (1974).

60. Rickard, L. J., P. Palmer, M. Morris, B. Zuckerman et al., Astrophys. J. Letters 199, L75 (1975).

61. Lynds, B. T., Astrophys. J. Suppl. Ser. 7/64, 1 (1962).

62. Walker, R. G., and S. D. Price, "AFCRL Infrared Sky Survey," AFCRL TR75-0373, 1975.

63. Rozhkovskiy, D. A., and A. V. Kurchakov, Trudy astrofiz. in-ta Kaz. SSR 11, 1 (1968).

ORIGINAL PAGE IS
OF POOR QUALITY

TABLE 1. DATA ON OBSERVATIONS OF OH, H_2CO, AND HI FEATURES IN DIRECTION OF CAS A, TAU A, AND CYG A [18]. /25

Source	V (km/sec)	$\int \tau_H dV$ (km/sec)	$\int \tau_{OH} dV$ (km/sec)	$\int \tau_{H_2CO} dV$ (km/sec)	$T_{kinet.}$ calc. prod.		$N_H \cdot 10^{20}$ (cm^{-2})	n_H (cm^{-3})	$N_{OH} \cdot 10^{13}$ (cm^{-2})	$n_{OH} \cdot 10^{-6}$ (cm^{-3})	$N_{H_2CO} \cdot 10^{11}$ (cm^{-2})	$n_{H_2CO} \cdot 10^{-3}$ (cm^{-3})
Cas A	+7.6	0.30	0.0011	<0.0015	-	100	0.55	1.8	0.25	0.08	<2.8	<0.9
	-0.4	2.96	0.050	0.017	99±24	100	5.4	18	11.2	3.7	4.8	1.6
	-1.9	1.75	0.040	0.019	47±17	50	1.6	5.3	9.0	3.0	5.4	1.8
	-6.6	0,65	0.0003	<0.0016	-	100	1.2	4.0	0.07	0.024	<2.5	<0.8
	-12.5	0.43	<0.0015	<0.0016	-	100	0.80	2.7	0.34	<0.11	<2.5	<0.8
	-34.1	2.05	0.0023	<0.0014	-	100	3.8	12.5	0.52	0.17	<2.1	<0.7
	-37.6	6.34	0.050	0.033	140±30	100	11.4	37	11.2	3.7	9.2	3.1
	-41.1	9.72	0.090	0.058	350±40	100	17.7	58	20.3	6.8	16.2	5.4
	-44.5	-	0.029	-	-	-	-	-	6.5	2.2	-	-
	-47.3	8.66	0.060	0.033	139±50	100	15.9	52	13.5	4.5	9.2	3.1
	-48.8	11.2	0.057	0.016	380±120	100	20.6	67	12.8	4.3	4.5	1.5

[see continuation of Table 1.]

ORIGINAL PAGE IS
OF POOR QUALITY

TABLE 1. (continued)

426

Source	V (km/sec)	$\int \tau_N dV$ (km/sec)	$\int \tau_{mw} dV$ (km/sec)	$\int \tau_{micro} dV$ (km/sec)	$T_{kinet.}$ calc.	pred.	$N_H \cdot 10^{20}$ (cm^{-2})	n_H (cm^{-3})	$N_{mw} \cdot 10^{19}$ (cm^{-2})	$n_{mw} \cdot 10^{-4}$ (cm^{-3})	$N_{micro} \cdot 10^{19}$ (cm^{-2})	$n_{micro} \cdot 10^{-4}$ (cm^{-3})
Tau A	+10.3	4.54	0.013	<0.002	27±20	50	4.2	14	2.9	0.97	<0.53	<0.14
	+3.9	2.22	0.0074	<0.003	-	-	2.4	8.1	0.83	0.28	<0.81	<0.27
	+2.9	1.90		<0.002	-	-	2.1	7.0	0.83	0.28	<0.70	<0.23
	-4.0	0.27	<0.0018	<0.0023	-	-	0.50	1.7	<0.4	<0.13	<0.89	<0.30
Cyg A	+3.2	1.27	0.027	0.005	180±40	100	2.3	7.5	6.1	2.0	1.3	0.43
	-0.0	0.82	<0.0063	<0.002	-	100	1.5	4.9	<1.4	<0.47	<0.53	<0.17
	-84.5	0.99	<0.0068	<0.005	-	100	1.8	5.8	<1.5	<0.51	<1.34	<0.45

ORIGINAL PAGE IS
OF POOR QUALITY

TABLE 2. SUPERNOVA REMNANTS WITH LARGE FLUXES AT 26MHz /27

Designation	α_{1950}			δ_{1950}		F_{26}	F_{400}	F_{1400}	F_{5000}	Ang. diam.	Diameter (ps)	z (ps)	Dist. (kps)	H 109
SN Tycho Brahe	00^h	22^m	28^s	$63°$	51'.9	500	100	42	21	7'.0	7.1	86	3.5	-
IC 443	06	14	08	22	49.0	850	250	130	75	45'	1.5			no
KE 19 A	13	43	33	-60	8.3	500	130		33	6'.3	10.7	178	5.8	no
KE 47 (CTB 37 B)	17	11	12	-38	26.7	500	124	74	39	7'.0	11.6	10	5.7	no
W 44	18	53	36	01	15.0	1000	390	215	149	32'	3.0			-
W 66	20	20	44	40	02.3	5000	620	250	100	8'.0	7.9	105	3.4	yes
Cas A	23	21	11	58	32.8	5×10^4	6400	2410	910	4'.0	4.0	-126	3.4	no

ORIGINAL PAGE IS
OF POOR QUALITY

TABLE 3. EXTRAGALACTIC SOURCES BRIGHT AT 25-26 MHz AND OBSERVATIONS OF THEM IN HI, OH, AND CO LINES. /28

No.	Designation	Identification radio	/opt.	F_{25-26}	A_{HI}	OH_{1667} $\tau\times10^{-3}$	V km/sec	ΔV km/sec	CO $T_A(K)$	V km/sec	ΔV km/sec	HI A	V km/sec	ΔV km/sec	Notes
I	2	3	4	5	6	7	8	9	I0	II	I2	I3	I4	I5	I6
I.	V 0I33+20	zs	47	QSO	I90	–									
2.	V 03I6+4I	zs	84	G	75I	0,2I									
3.	Gr 0356+I0	zs	98	G	232	0,40									
4.	V 04I5+37	zs	III	G	334	0,2I	I80	-I,0	2,6	6,I	-2,0	2,9	0,65	-I,I	7,6	zs III OB
										9,8	-I,9	3,8	0,65	-I,I	7,6	zs III OA
5.	V 0433+29	zs	I23	G	828	0,28									
						0,89	60	4,5	2,5							
6.	V 0445+44	zs	I29,0		(230)	0,76	86	-25,5	0,9	2,I	-25,8	I,4	0,48	-27	3,5	
						0,48										
						0,38										
						0,57										
						0,34										

[see continuation of Table 3.]

TABLE 3. (continued)

/29

I	2	3	4	5	6	7	8	9	I0	II	I2	I3	I4	I5	I6
7.	V 050I+37	zs	I34	469	0,40										
					0,54										
					0,80										
					0,54										
					0,68										
8.	Gp 0625-05	zs	I6I	G 2I9	0,55	I3	8,6	I,I							OH-[30,26]
					0,I3	I2	7,5	2,5							
9.	V 08I0+48	zs	I96	Q 2I8	0,07										
I0.	V 09I8+45	zs	2I9	G 2I2	-										
II.	Gp I226+02	zs	279	Q 238	-										
I2.	V I502+26	zs	3I0	G 382	0,29										
I3.	Gp I5I5+07	zs	3I7	G 227	-										
I4.	Gp I600+02	zs	327	G 203	0,I7										
I5.	V I627+39	zs	338	G 3I4	-										
I6.	Gp I7I7+00	zs	353	G 8I0	0,73	36	0,2	I,4							OH-[26]
					0,06										

[see continuation of Table 3.]

TABLE 3. (continued)

/30

2	3	4	5	6	7	8	9	I0	II	I2	I3	I4	I5	I6
V I8I8+48	3C 380	Q	27I	0,09										
V 20I2+23	3C 409		38I	0,30	I9	I5,4	0,7	2,I	I3,3	I,2				
				0,64										
V 2I2I+24	3C 433	G	267	0,27										
V 2I53+37	3C 438	G	228	0,64										
				0,44										
V 2243+39	3C 452	G	288	0,07										
				0,03										

NOTES: F_{25-26} fluxes taken from [9-13];
A_{HI} -- [25]; data on OH observations -- pp.7-9 -- [30, 40, 44];
HI -- pp. 13-15 -- [26];
commas in numerals indicate decimal points.

ORIGINAL PAGE IS
OF POOR QUALITY

TABLE 4. QUASARS WITH ABSORPTION OPTICAL SPECTRA AND RELATIVELY LARGE FLOWS OF RADIATION AT LOW FREQUENCIES

/31

No.	Designation	z_e	ν	$F_{\nu min}$ (J)	Notes
I	3CR9 (0017+15)	2.012	26	100	
2	PKS 0019-046	1.948	80	11	
3	PKS 0454-220	0.534	80	16	
4	0835+580	1.534	26	61	
5	0955+326	0.533	26	27	
6	3C232 (B2 1218+339)	1.519	26	61	Paired with NGC 3067; 21 cm
7	PKS 1229-021	1.038	26	≈15	Flux extrapolated from 178 MHz according to data from [51]; 21 cm
8	3C286 (B2 1328+30.7)	0.849	26	34	21 cm
9	PKS 1354+195	0.720	26	38	
10	1421+33.0	1.904	26	54	
11	PKS 1458+718	0.905	38	40	
12	PKS 2223-052 (3C 446 - BL Lac object)	1.404	26	≈45	Flux extrapolated from 80 MHz according to data from [51]

TABLE 5. DARK REGIONS IN LYNDS' CATALOG AND IR SOURCES AND REFLECTING NEBULAE ASSOCIATED WITH THEM /32

No.	l	l^{II}	b^{II}	α_{1950}	δ_{1950}	Region in quad. degr.	Degree of opacity	IR Source α_{1950}	IR Source δ_{1950}	Reflecting nebula
I	2	3	4	5	6	7	8	9	I0	II
I.	L 317	11°.89	20°.40	$16^h\ 58^m.0$	-8°00′	I.600	4			
2.	L 368	15°.82	4°.18	$18^h\ 2^m.5$	-13°10′	I.550	4			
3.	L 406	19.40	0.44	18 23.0	-11 50	0.746	5	$18^h\ 24^m\ 47^s$	-12° 0′.0	
4.	L 434	21.64	-3.08	18 40.0	-11 30	I.II	4			
5.	L 435	21.83	-0.21	18 30.0	-10 00	8.40	4	18 28 50	-9 38.2	IC I287
								18 28 55	-10 0.3	
								18 30 53	-9 10.7	
								18 31 37	-11 33.3	
								18 32 02	-8 36.1	
6.	L 444	22.70	8.70	16 00.0	-5 00	I.030	4	18 04 01	-4 54.2	
7.	L 547	29.29	-1.35	18 48.0	-3 55	2.300	4			
8.	L 548	29.32	-1.06	18 47.0	-3 45	I.000	5	18 49 45	-3 47.8	

[see continuation of Table 5.]

TABLE 5. (continued) /33

I	2	3	4	5	6	7	8	9	I0	II
9.	L 559	29°.80	3°.97	$18^h\ 30^m.0$	-1°00′	I7.000	4	$18^h\ 34^m\ 44^s$	-2° 43′.1	I) $\alpha = 18^h\ 32^m.3$
								18 39 31	-2 49.6	$\delta = 0°00'$
I0.	L 572	30°.46	4°.88	$18^h\ 28^m.0$	0° 00′	I4.000	4	18 24 31	I 6.8	2) $\alpha = 18^h\ 27^m.9$
								18 27 44	-I 24.2	$\delta = 1°11'$
								18 28 47	-2 7.6	3) $\alpha = 18^h\ 28^m.5$
										$\delta = 1°21'$
II.	L 628	36°.67	0°.21	18 56.0	3. 22	2.000	4	18 55 13	3 22.9	
								18 59 14	4 7.7	
I2.	L 669	45°.47	3.65	19 0.0	I2. 45	I.280	4	19 00 56	I2 9.5	
I3.	L 716	51.60	I.I4	19 21.0	I7 00	I4.00	4	19 19 25	I7 33.9	
I4.	L 741	54.90	3.45	19 19.0	21 00	7.00	4	19 14 37	21 48.7	I) $\alpha = 19^h\ 24^m.2$
										$\delta = 22°40'$
								19 17 32	22 27.1	2) $\alpha = 19^h\ 22^m.07$
										$\delta = 22°37'$
I5.	L 935	84.79	-0.88	20 55.0	43 40	2.250	4	20 56 19	44 35.4	
I6.	L I472	I60.39	-19.17	3 38.0	31 0	3.580	4	-	-	IC 348
I7.	L I52I	I72.60	-14.83	4 30.0	26 0	4.I00	4	4 27 55	27 24.1	
I8.	L I534	I74.05	-13.95	4 37.0	25 30	0.870	5	-	-	

[see continuation of Table 5.]

OF POOR QUALITY

ORIGINAL PAGE IS
OF POOR QUALITY

~~ORIGINAL PAGE IS~~
~~OF POOR QUALITY~~

TABLE 5. (continued)

/34

I	2	3	4	5	6	7	8	9	I0	II
I9.	L I538	I75°.34	-I3°.23	4^h $43^m.0$	25°.0′	3.000	4			
20.	L I605	20I.24	0.52	6 30.0	I0′.40	I.250	4			Nec 2247
2I.	L I630	206.02	-I5.29	5 43.0	-I 0	5.980	4	5^h 39^m 06^s	-2° I7′.0	
								5 39 I2	-I 58.9	Nec 2064
								5 44 29	0 I8.I	
22.	L I64I	2I0.64	-I9.83	5 35.0	-7 0	6.270	4	05 37 I9	-8 II.I	

ORIGINAL PAGE IS
OF POOR QUALITY

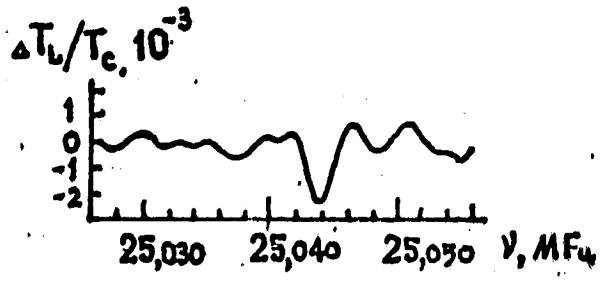

Fig. 1a. Profile of C640α line in the direction of Cas A [3].

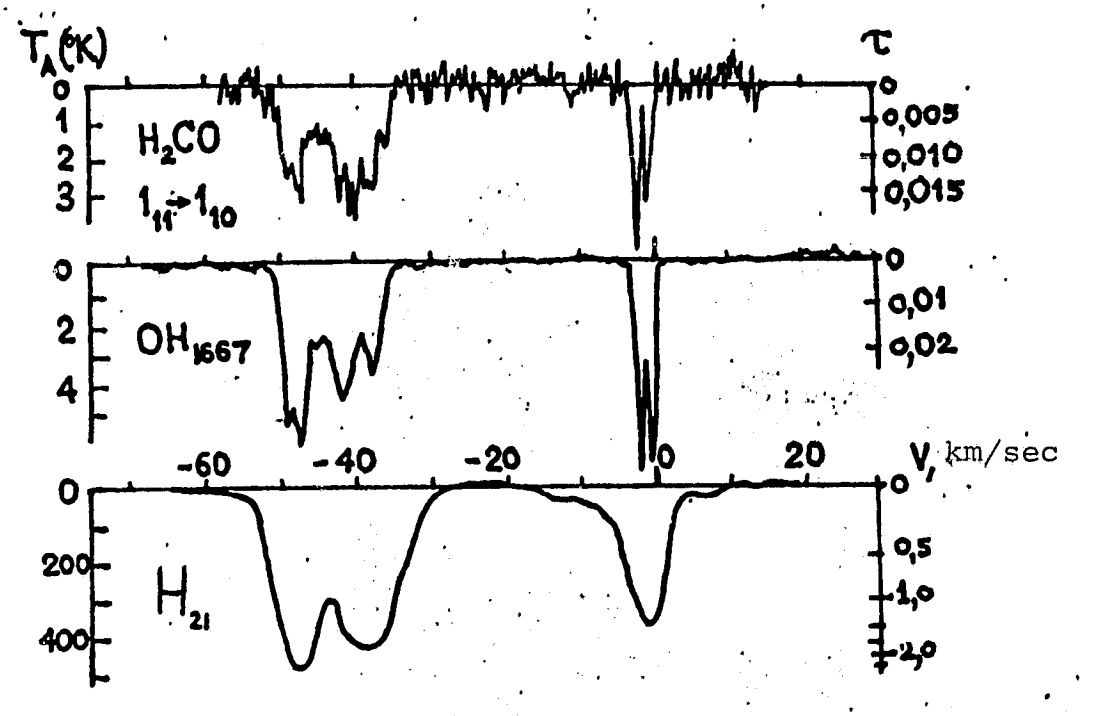

Fig. 1b. Profile of neutral hydrogen and molecular lines in the direction of Cas A, obtained at Jodrell Bank and at NRAO; illustration from [18].

ORIGINAL PAGE IS
OF POOR QUALITY

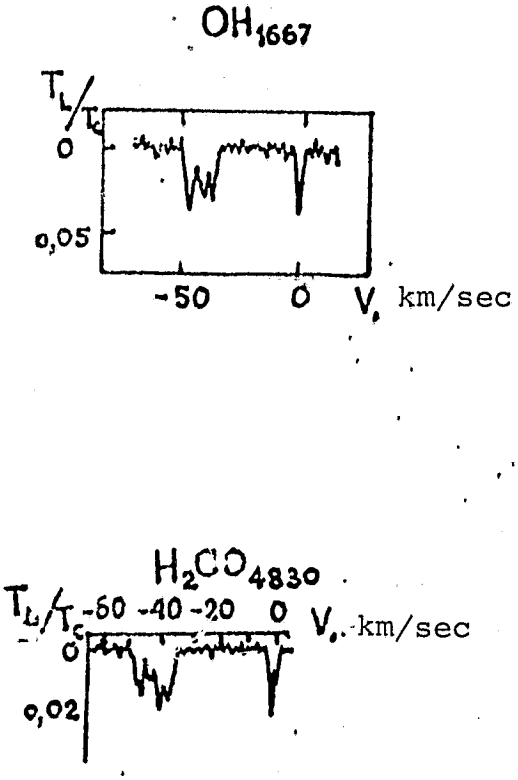

Fig. 1c. OH and H_2CO in direction of Cas A (Eifelsberg) [19].

ORIGINAL PAGE IS
OF POOR QUALITY

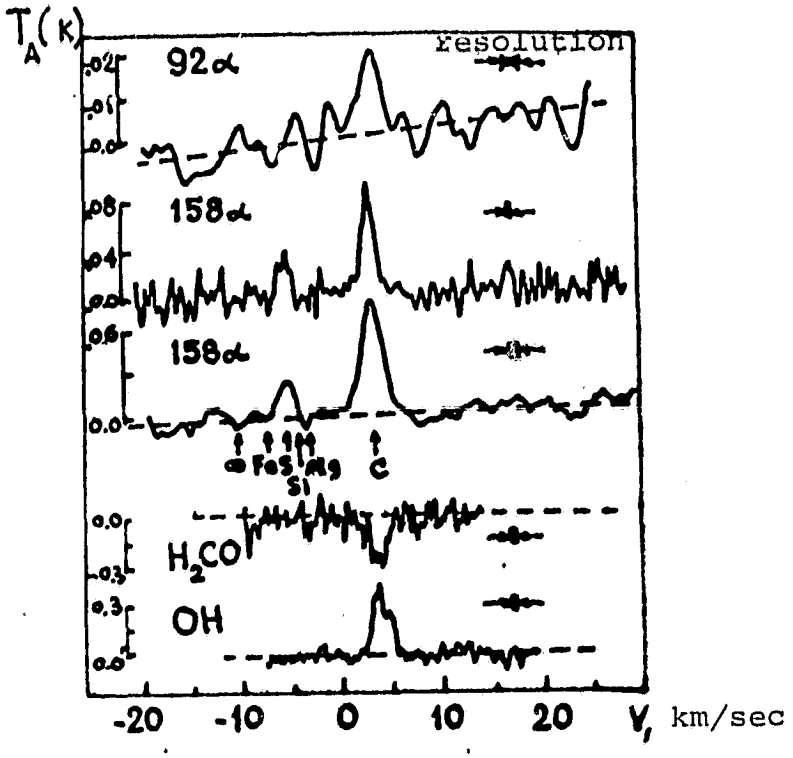

Fig. 2. Recombination and molecular spectra in the direction of ρ Oph [17].

ORIGINAL PAGE IS
OF POOR QUALITY

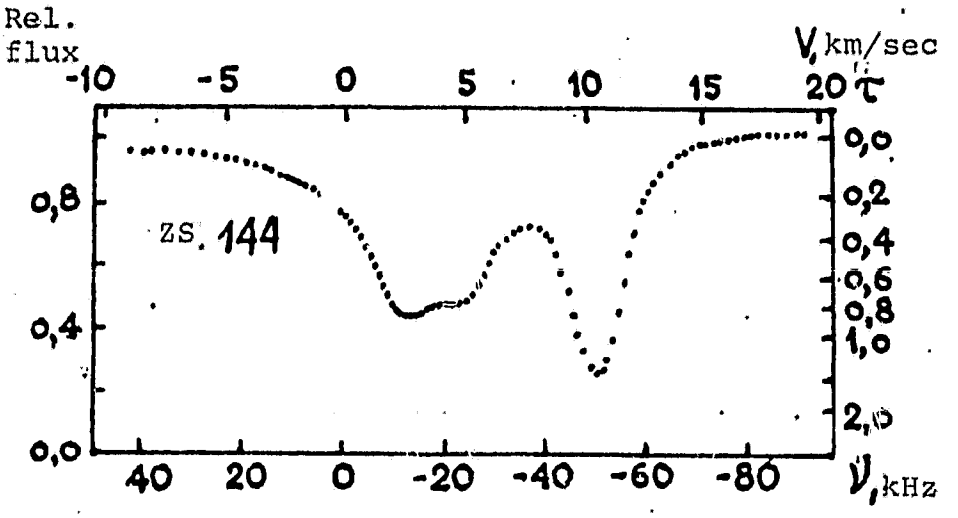

Fig. 3. HI 21 cm in direction of Tau A [23]

ORIGINAL PAGE IS
OF POOR QUALITY

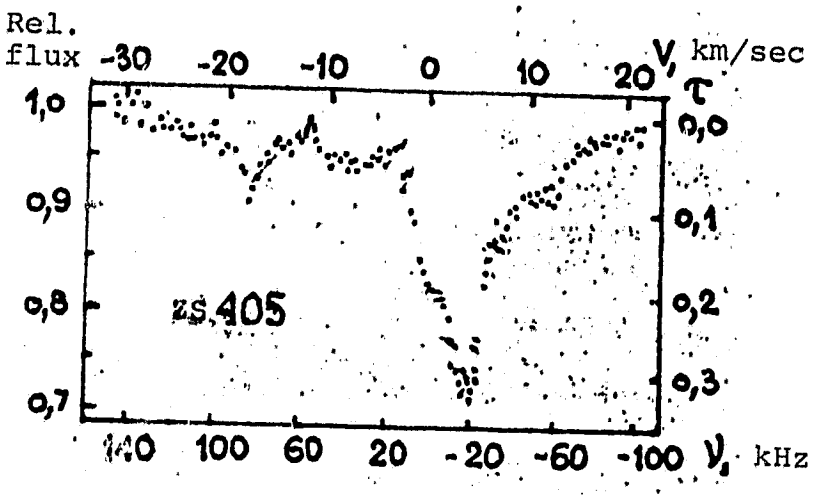

Fig. 4a. HI 21 cm in direction of Cyg A in the zero velocity region [23].

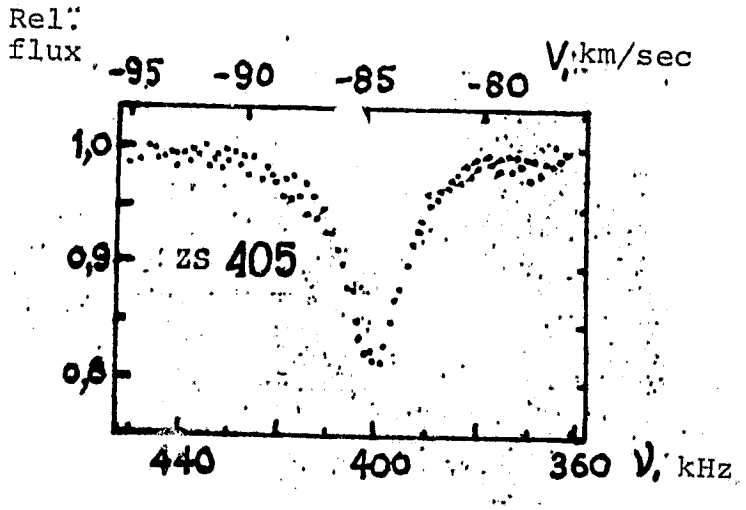

Fig. 4b. HI 21 cm in direction of Cyg A -- Persean Arm [23].

ORIGINAL PAGE IS
OF POOR QUALITY

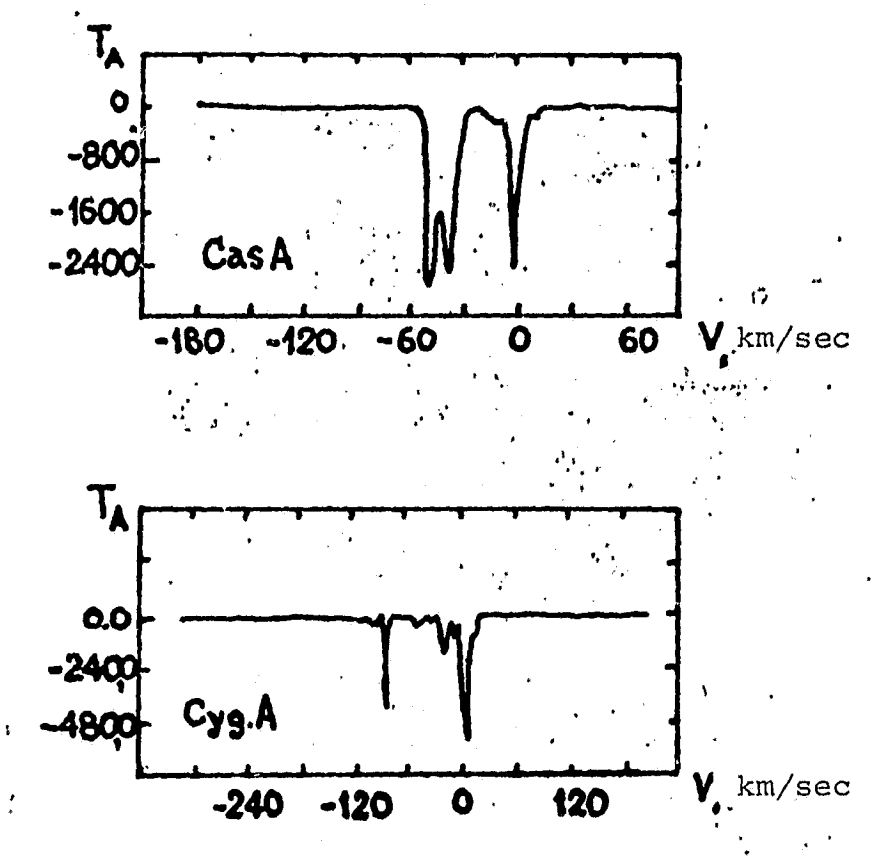

Fig. 4c. Absorption in HI 21 cm line in direction of Cas A and Cyg A -- Bonn radio telescope [24].

ORIGINAL PAGE IS
OF POOR QUALITY

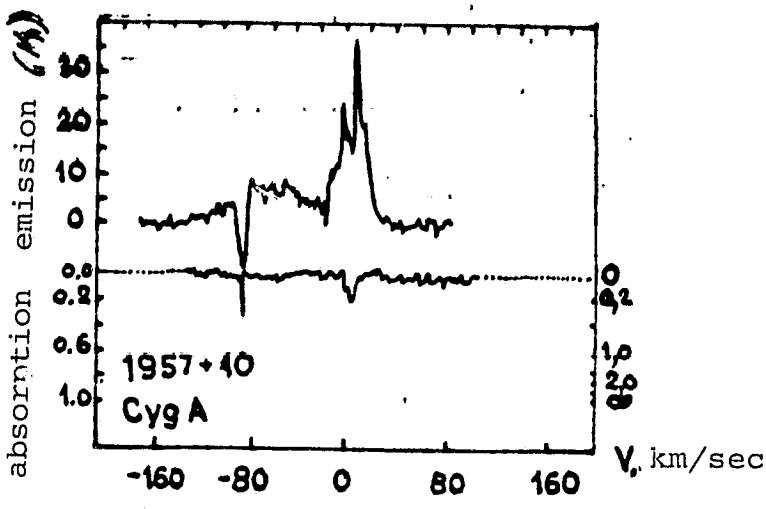

Fig. 4d. Emission and absorption in HI (21 cm) line in direction of Cyg A -- Nantes [25].

OF POOR QUALITY

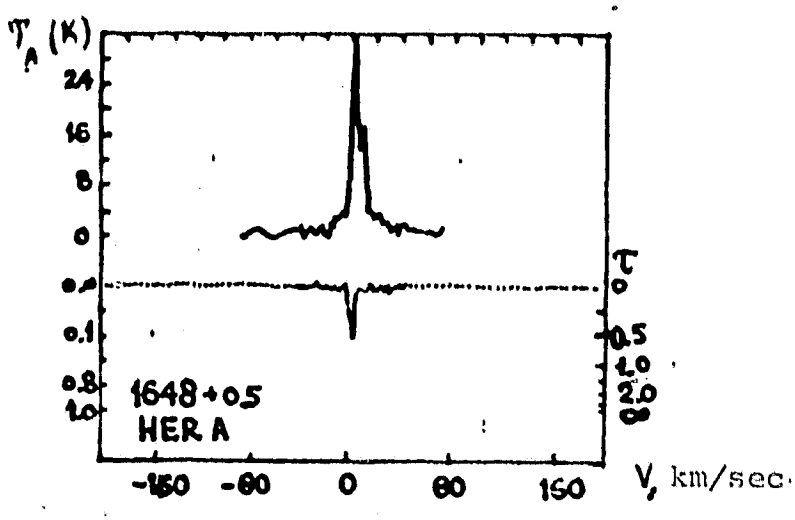

Fig. 5a. Emission and absorption in HI (21 cm) line in direction of Her A -- Nantes [25].

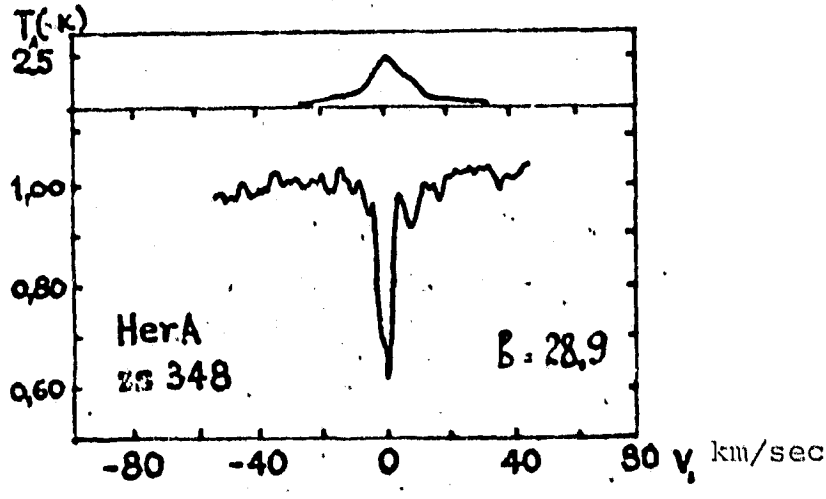

Fig. 5b. Emission and absorption in HI (21 cm) line in direction of Her A with double antenna interferometer [28].

ORIGINAL PAGE IS
OF POOR QUALITY

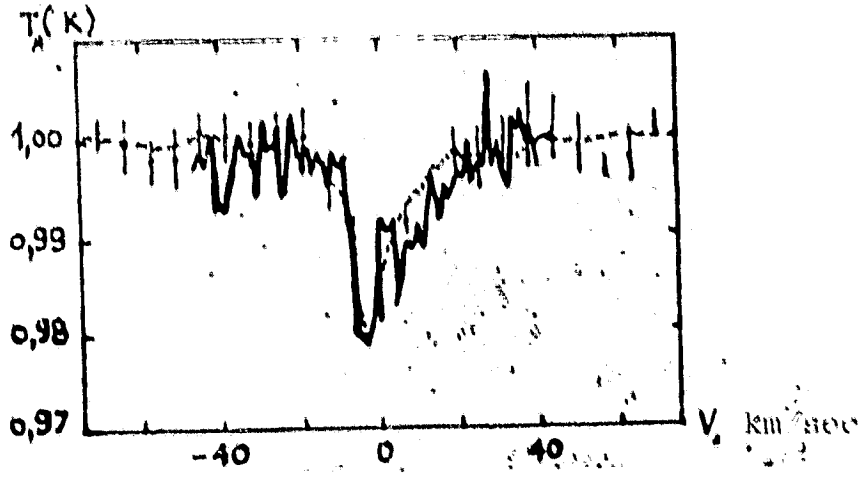

Fig. 6a. Profile of HI (21 cm) line in direction of Hyd A [27] -- Nantes.

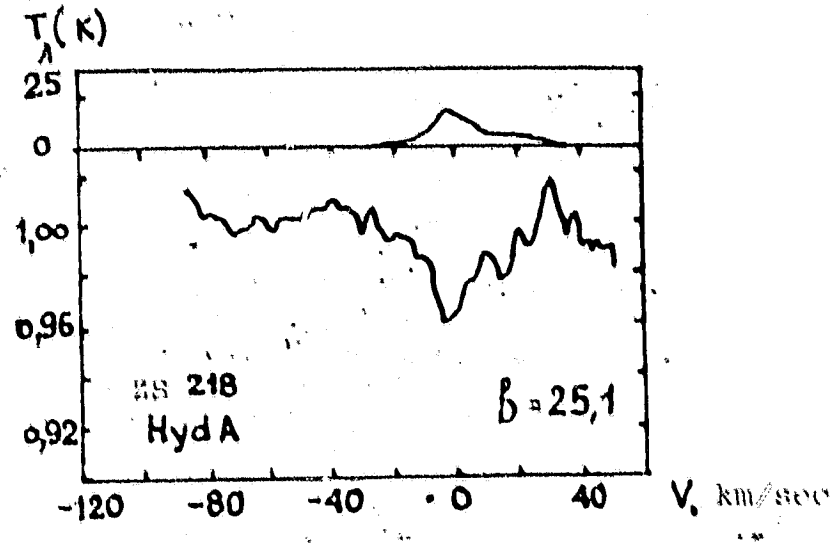

Fig. 6b. HI 21 cm at Hyd A, according to data from [28] -- double antenna interferometer.

ORIGINAL PAGE IS
OF POOR QUALITY

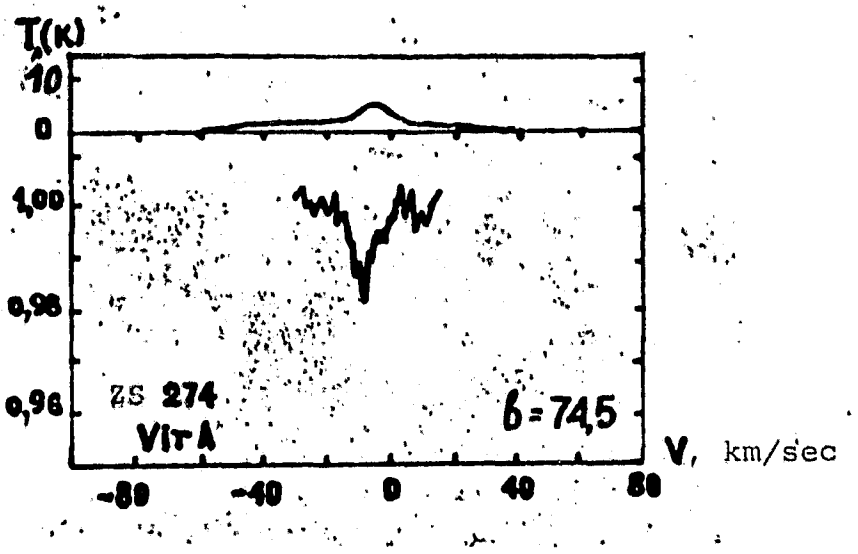

Fig. 7. HI 21 cm in direction of Vir A [28].

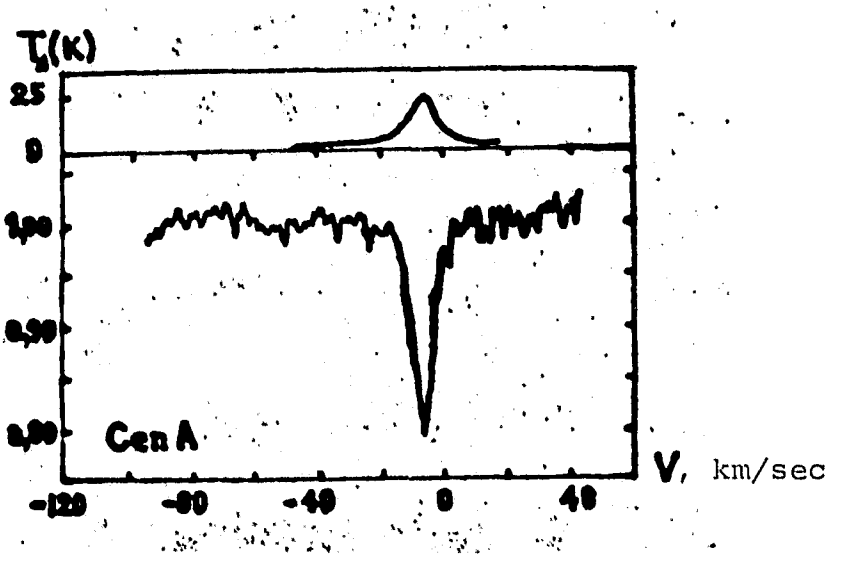

Fig. 8. Absorption at 21 cm in direction of Cen A [28].

ORIGINAL PAGE IS
OF POOR QUALITY

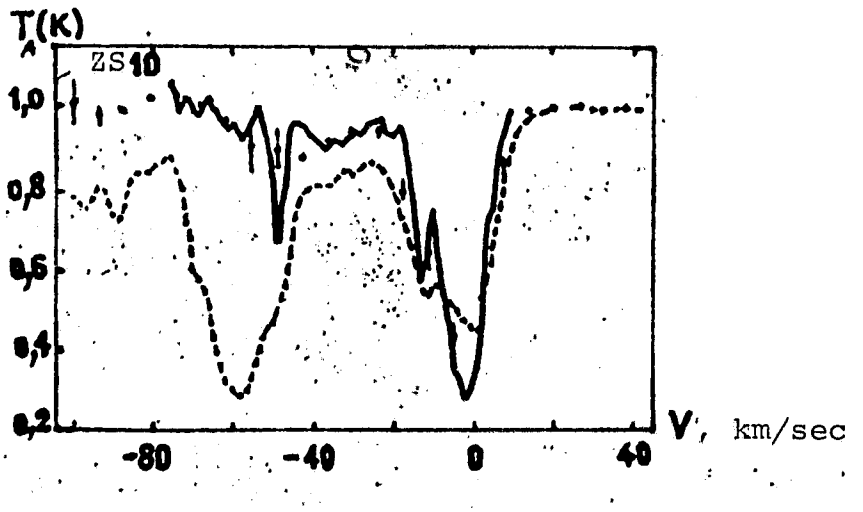

Fig. 9a. Profile of HI 21 cm line in direction of SNR Tycho Brahe, obtained at Nantes [27].

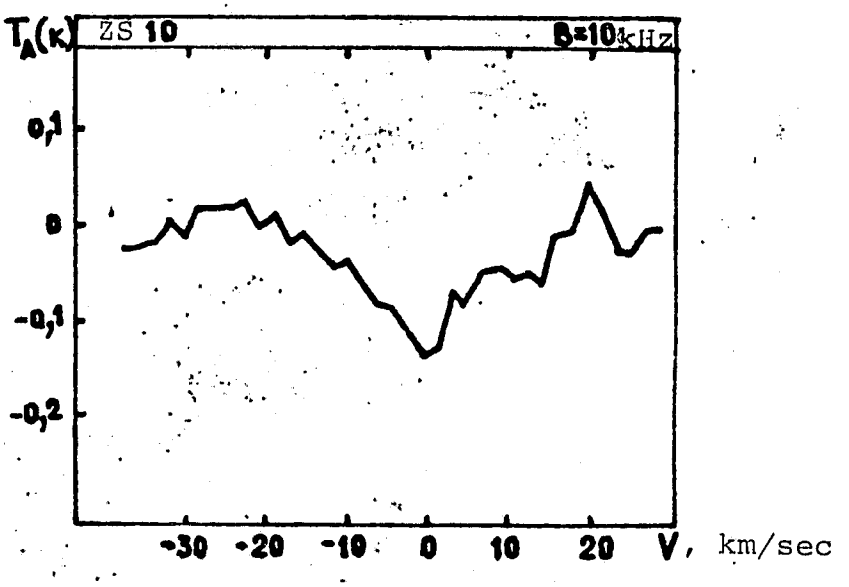

Fig. 9b. Profile of OH_{1667} line in direction of SNR Tycho Brahe, obtained at Nantes with a resolution of 10 kHz [40].

ORIGINAL PAGE IS
OF POOR QUALITY

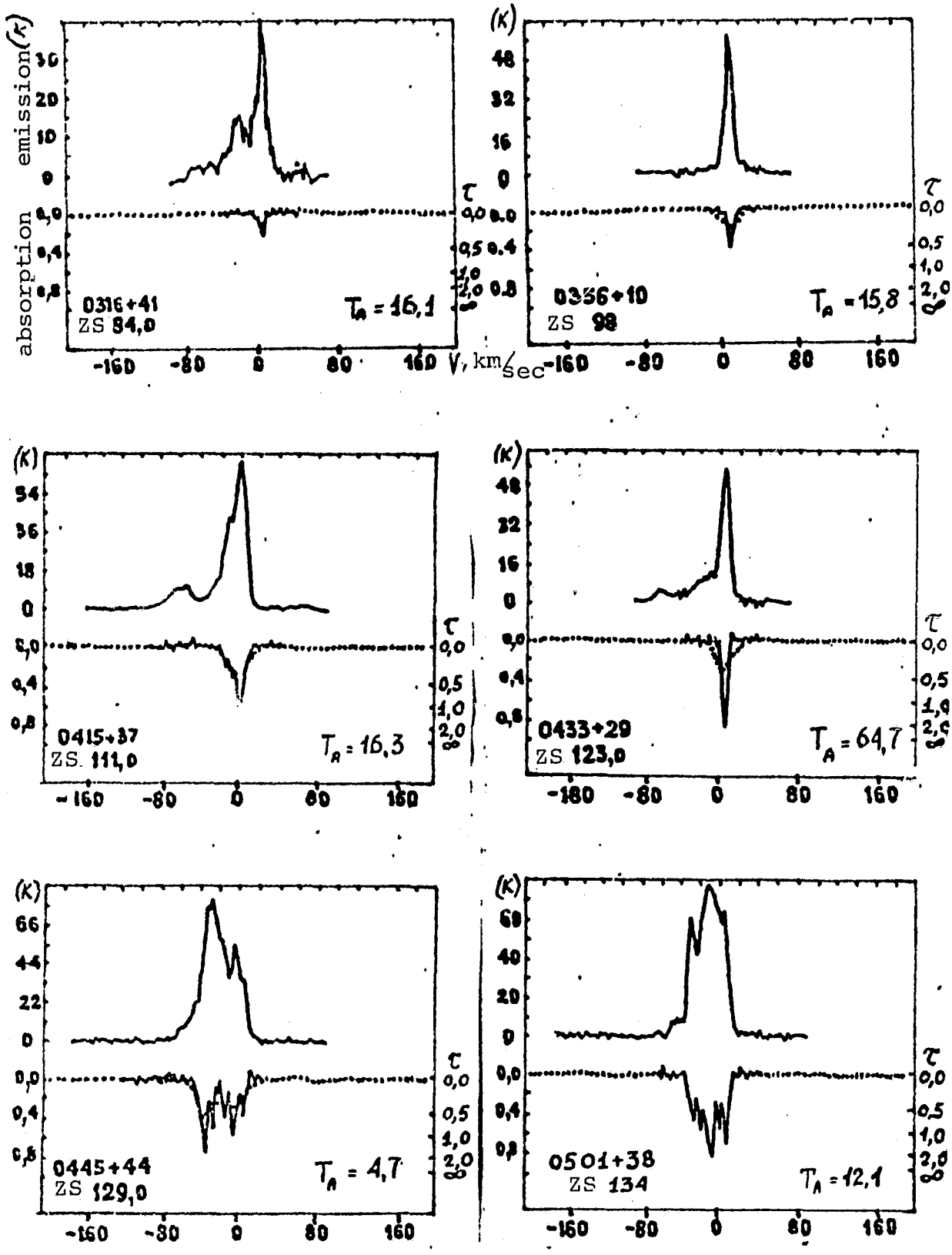

Fig. 10. Absorption and emission spectra [25] of extra-galactic radio sources bright at 26 MHz in HI 21 cm line.

ORIGINAL PAGE IS
OF POOR QUALITY

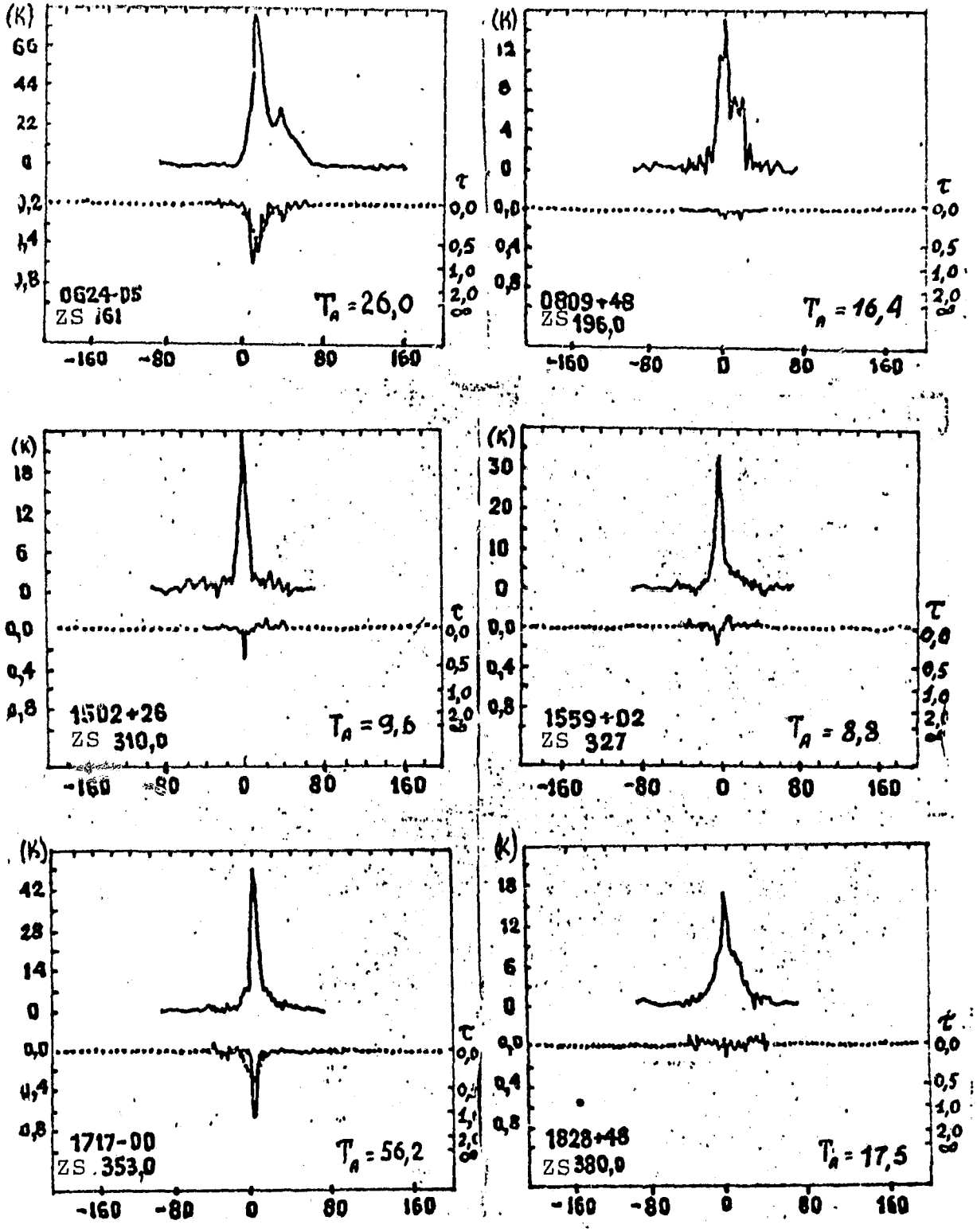

Fig. 10 (continued).

ORIGINAL PAGE IS
OF POOR QUALITY

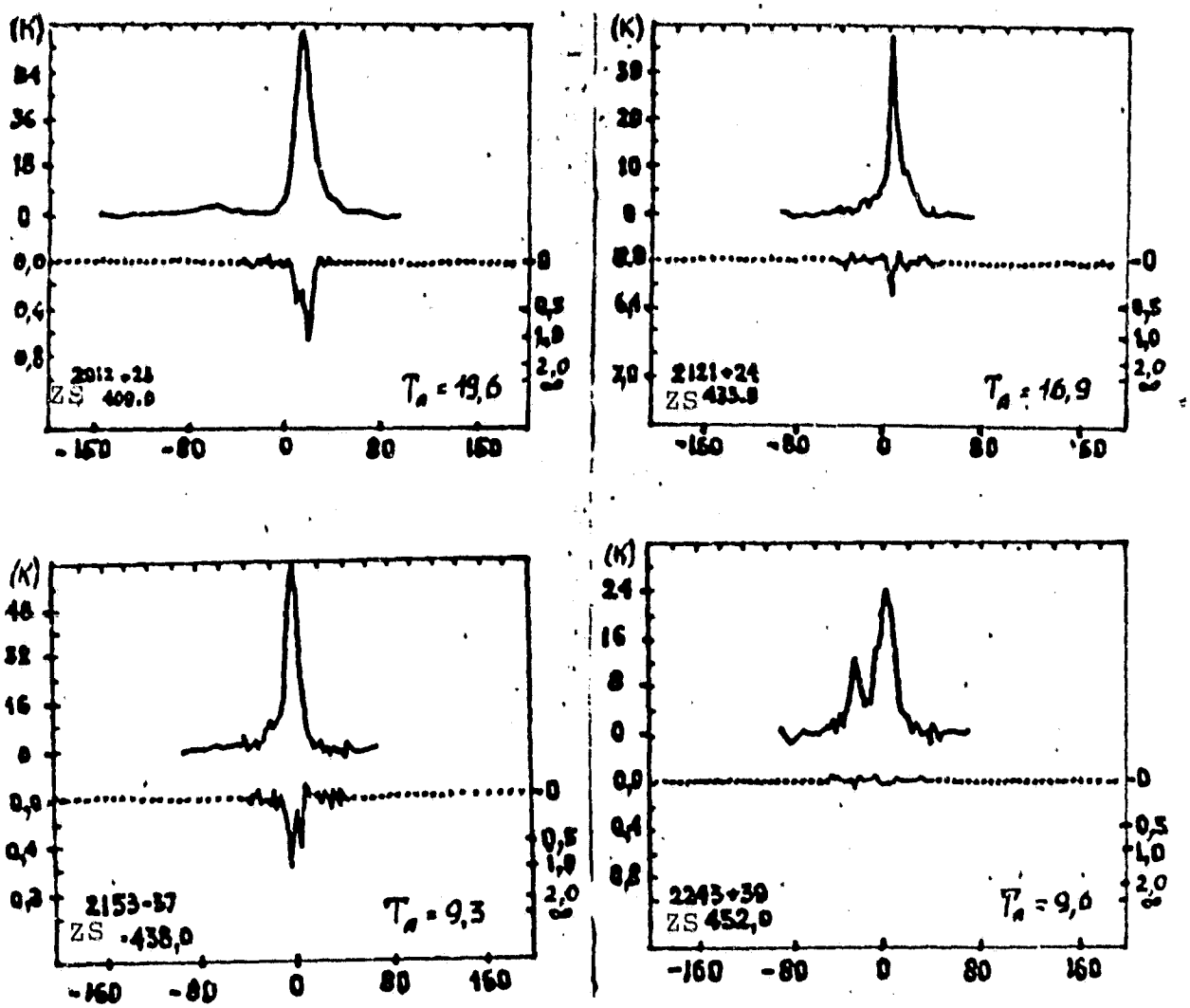

Fig. 10 (continued).

ORIGINAL PAGE IS
OF POOR QUALITY

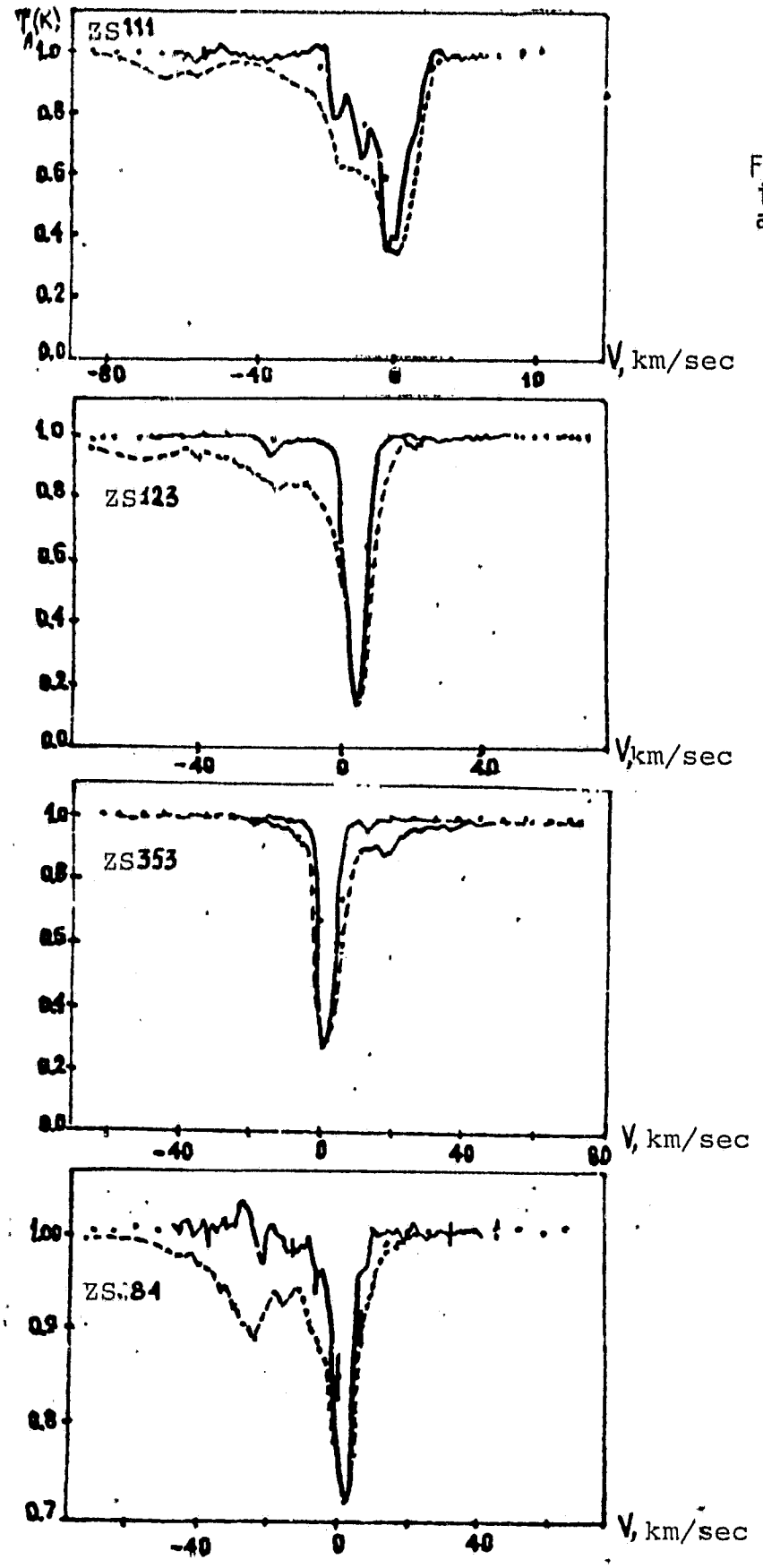

Fig. 11. Absorption spectra in HI 21 cm line, obtained at Nantes [27].

ORIGINAL PAGE IS
OF POOR QUALITY

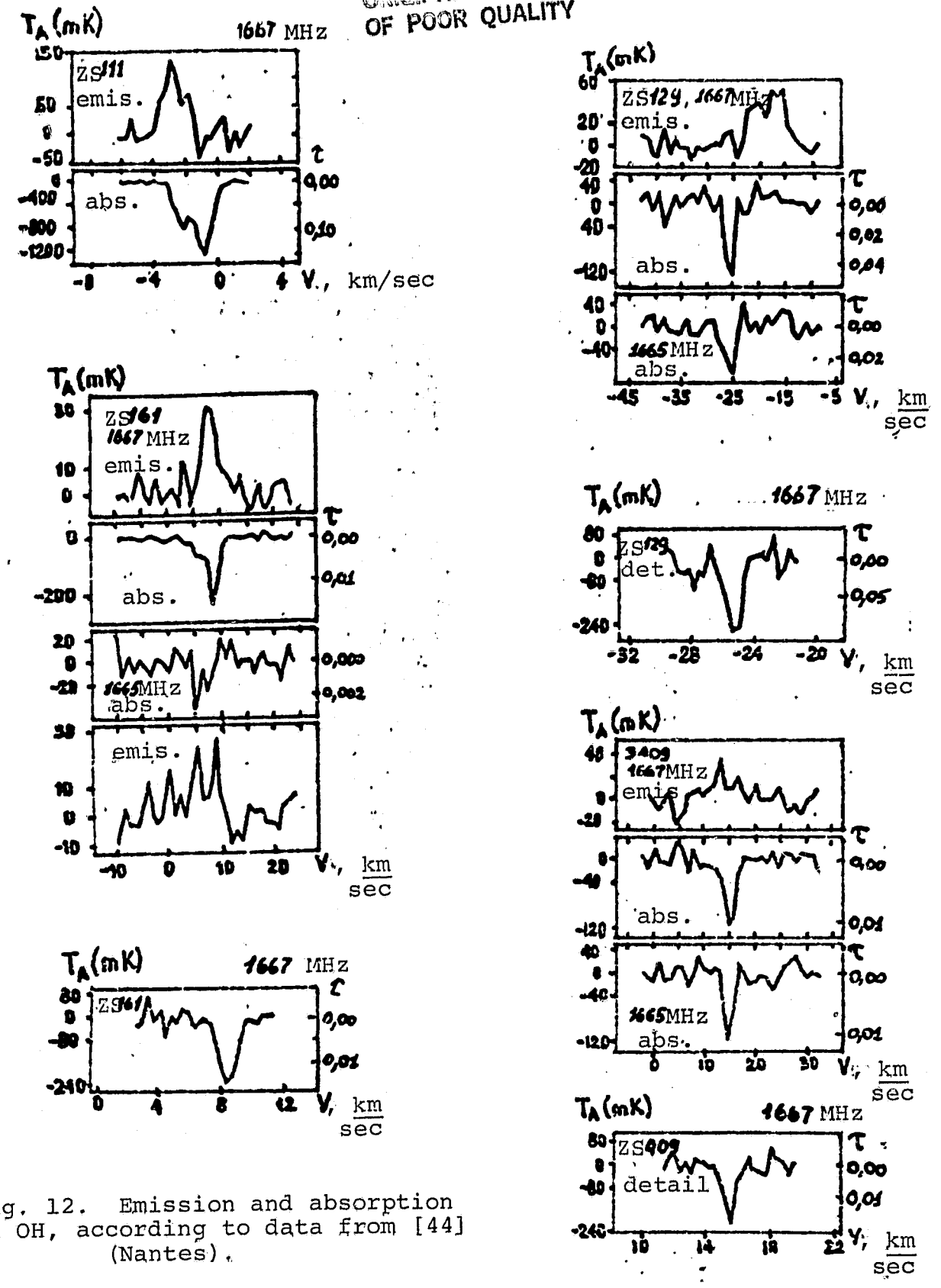

Fig. 12. Emission and absorption in OH, according to data from [44] (Nantes).

ORIGINAL PAGE IS
OF POOR QUALITY

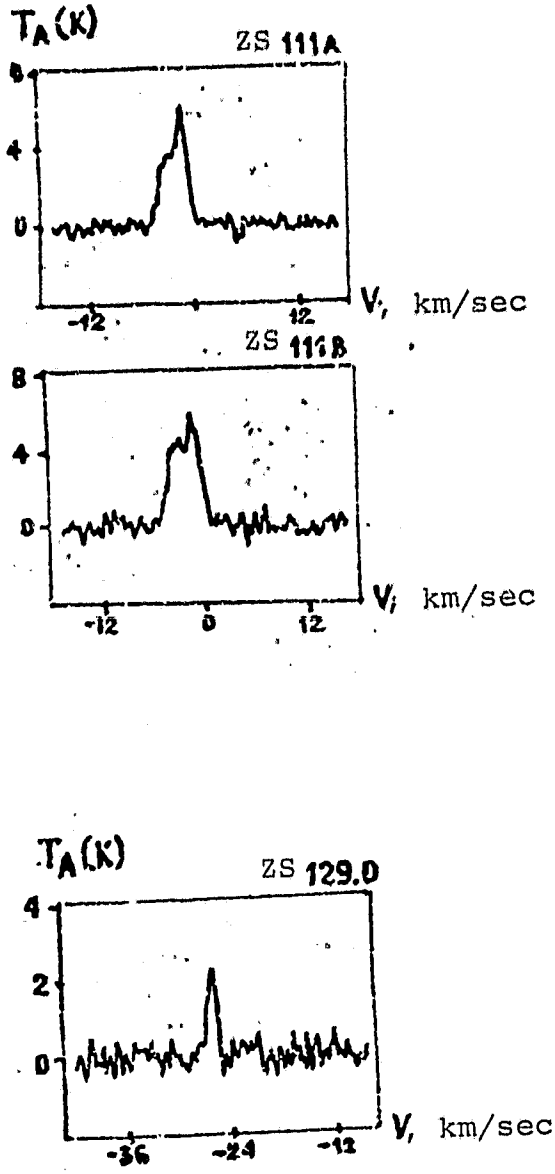

Fig. 13a. CO at 2.6 mm, according to data from [45] (Kitt Peak 11 m telescope).

ORIGINAL PAGE IS
OF POOR QUALITY

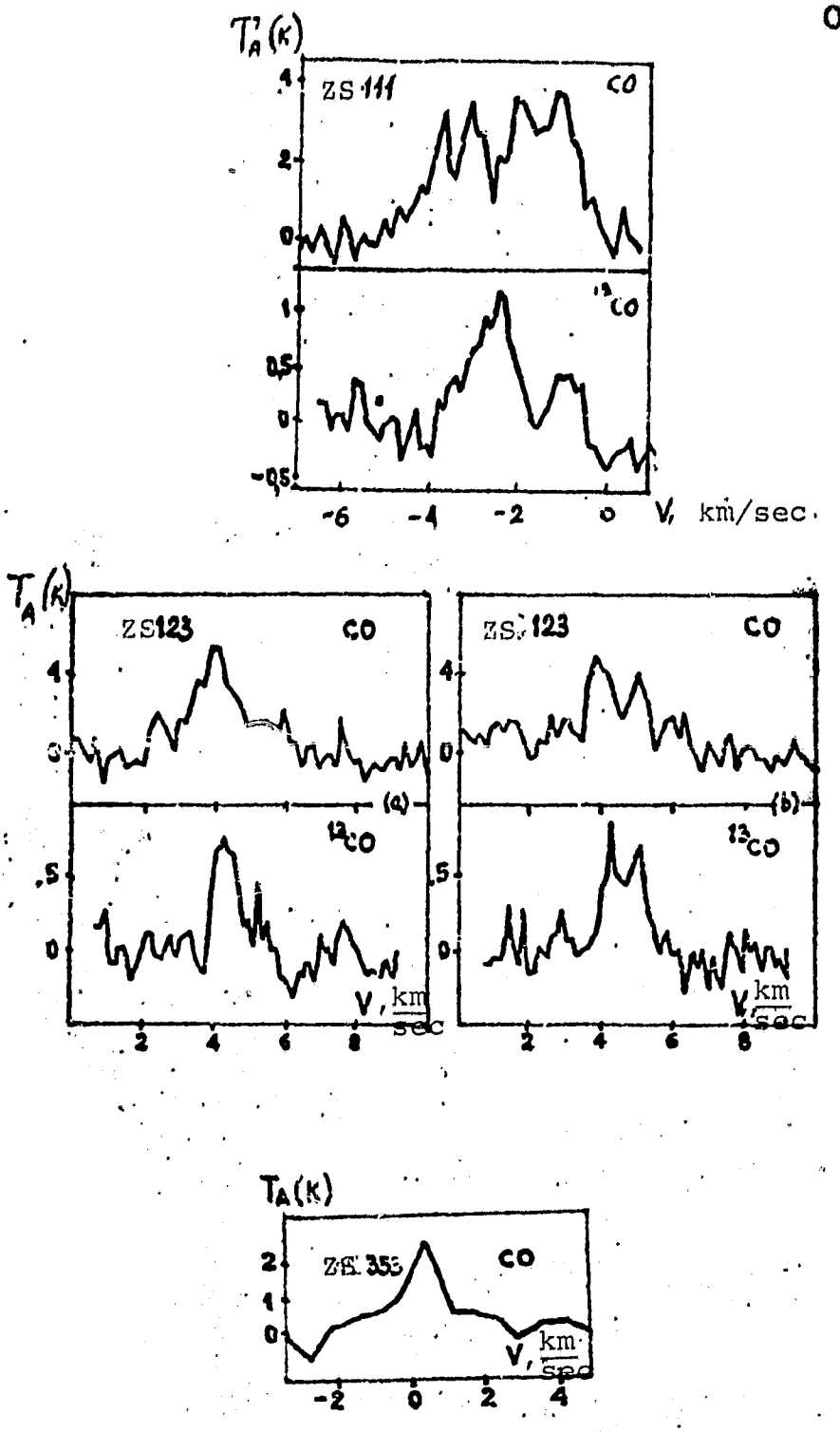

Fig. 13b. CO line ($J = 1 \rightarrow 0$) [48] --
(Fort Davis Observatory, 4.8 m antenna).

ORIGINAL PAGE IS
OF POOR QUALITY

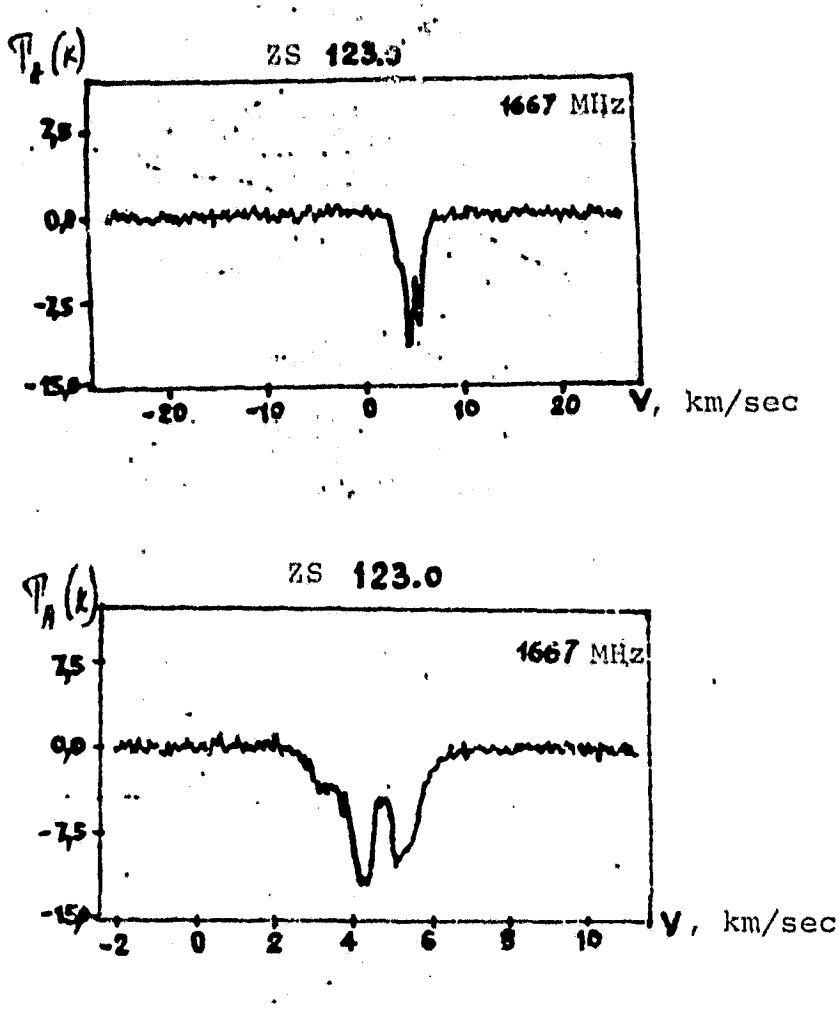

Fig. 14a. Profile of OH_{1667} line in direction of ZS 123, obtained at Arecibo [29].

ORIGINAL PAGE IS
OF POOR QUALITY

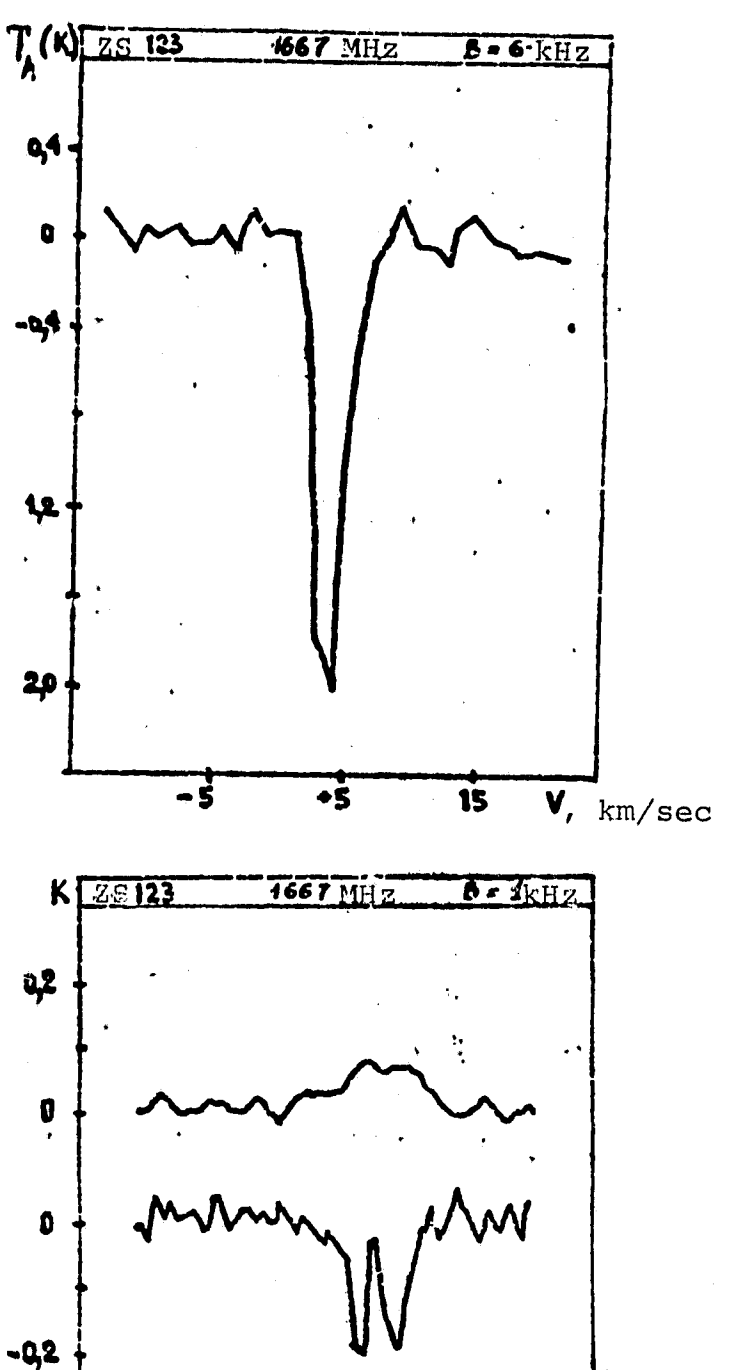

Fig. 14b. OH_{1667} in direction of ZS 123 [40]. Top -- at Nantes; bottom -- at Onsal.

ORIGINAL PAGE IS
OF POOR QUALITY

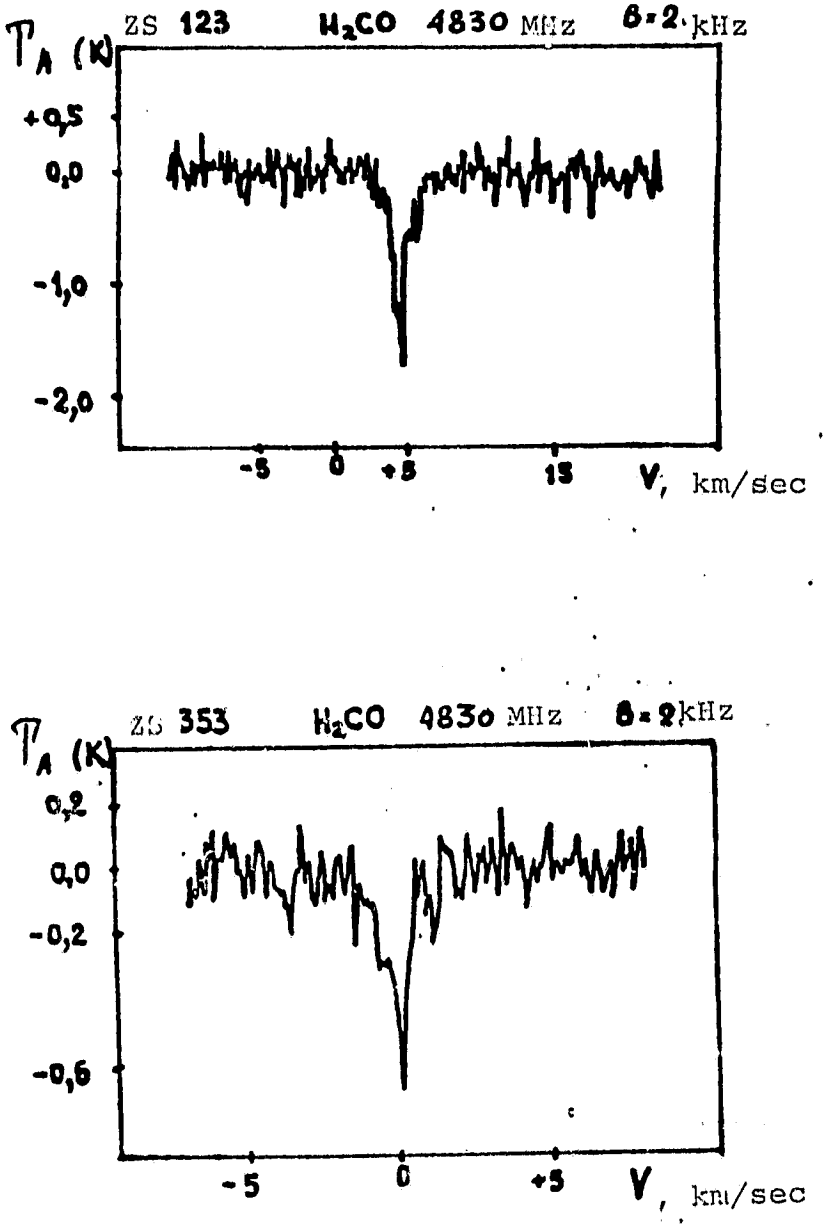

Fig. 15. Absorption in formaldehyde line in direction of ZS 123 and ZS 353 (Effelsberg [40]).

ORIGINAL PAGE IS
OF POOR QUALITY

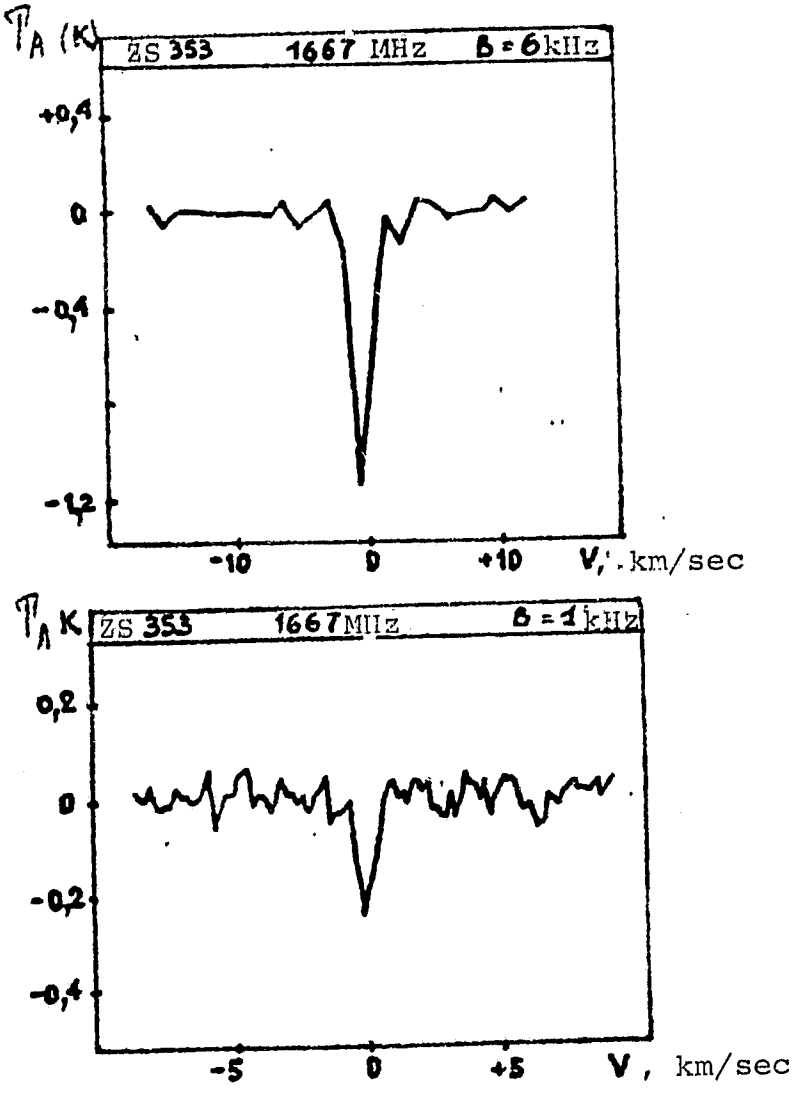

Fig. 16. OH_{1667} in direction of ZS 353 [40]; top -- at Nantes, bottom -- at Onsal.